# Holocene carbon accumulation in the peatlands of northern Scotland

J.L. Ratcliffe[1,2], R.J. Payne[3,4], T.J. Sloan[3], B. Smith[5], S. Waldron[5], D. Mauquoy[6], A. Newton[7], A.R. Anderson[8], A. Henderson[9] and R. Andersen[1]

[1]Environmental Research Institute, University of the Highlands and Islands, Thurso, Scotland, UK
[2]Science & Engineering, University of Waikato, Hamilton, New Zealand
[3]Environment Department, University of York, England, UK
[4]Department of Zoology and Ecology, Penza State University, Penza, Russia
[5]School of Geographical and Earth Sciences, University of Glasgow, Scotland, UK
[6]School of Geosciences, The University of Aberdeen, Scotland, UK
[7]School of GeoSciences, Institute of Geography, University of Edinburgh, Scotland, UK
[8]Forest Research, Northern Research Station, Roslin, Midlothian. Scotland, UK
[9]School of Geography, Politics and Sociology, Newcastle University, Newcastle upon Tyne, England, UK

## SUMMARY

The response of peatland carbon accumulation to climate can be complex, with internal feedbacks and processes that can dampen or amplify responses to external forcing. Records of carbon accumulation from peat cores provide a record of carbon which persists as peat over long periods of time, demonstrating the long-term response of peatland carbon stocks to climatic events. Numerous records of long-term carbon accumulation exist globally. However, peatlands from oceanic climates, and particularly blanket bog, remain under-represented. Scottish bogs, which collectively have more than 475 separate palaeoecological records, may prove to be a valuable resource for studying the impact of environmental change on past rates of carbon accumulation. Here we present 12 records of carbon accumulation from the north of Scotland. We support these results with a further 43 records where potential carbon accumulation is inferred from published ages. These reveal a trend of high carbon accumulation in the early Holocene, declining in the mid-to-late Holocene. The trend is consistent with accumulation profiles from other northern peatlands and is likely to have been caused by climatic cooling. Considerable variability in carbon accumulation rates between locations is apparent for the mid-to-late Holocene. We attribute to hydrologically induced changes in carbon accumulation which are likely to be inconsistent between sites.

**KEY WORDS:** blanket bog, Caithness, climate, Flow Country, LORCA, peat, Sutherland, tephrochronology

## INTRODUCTION

Global peatlands store carbon (C) equivalent to approximately two thirds of that contained within the atmosphere (Page & Baird 2016). Over the course of the 21st century, it is projected that peatlands will be subject to increased warming with changes in precipitation (Frolking *et al.* 2011). Large areas of peatlands have undergone or are undergoing significant changes in vegetation cover, most likely due to changing climate. For example, shrub cover has expanded across major areas of northern peatland (Klein *et al.* 2005, Hedwall *et al.* 2017) and tree cover across some continental peatlands (Pellerin & Lavoie 2003, Berg *et al.* 2009, Blanchet *et al.* 2017, Hedwall *et al.* 2017, Ratcliffe *et al.* 2017). Blanket bog, which requires a cool and moist climate, may be particularly vulnerable to change and is predicted to undergo a 50–59 % reduction in bio-climatic space by 2050 (Gallego-Sala & Prentice 2013).

Peatland vegetation can take several decades to respond to external forcing (Laine *et al.* 1995). The response of peatlands to climate and disturbance is complex (Belyea & Baird 2006, Belyea, 2009), with autogenic feedbacks (Waddington *et al.* 2015) which can play out over a period of centuries or more (Swindles *et al.* 2012, 2016). Thresholds of response to change are important, and highly site and time specific (Belyea 2009). Some climate events produce consistent and synchronous changes in vegetation, while others are inconsistently recorded in the peat stratigraphy (Mauquoy & Barber 2002, Mauquoy *et al.* 2002, Langdon & Barber 2004). The apparent resilience of the contemporary peatland carbon sink to recent climate change, observed across many peatlands globally (e.g. Sulman *et al.* 2009, Flanagan & Syed 2011, Goodrich *et al.* 2017), is not guaranteed to continue. The strong feedbacks inherent in peatlands must be considered in order to project their response to global change (Dise 2009).

Measurements of carbon accumulated within peat can provide a measure of how much carbon has been fixed and persisted over a period of centuries or more. Scottish bogs are thought to contain 1620 Mt of carbon (Chapman *et al.* 2009), a substantial proportion of the global blanket bog carbon pool. Scottish peatlands are also extensively studied, with more than 475 separate palaeoecological records (Ratcliffe & Payne 2016) which may prove to be a valuable resource for studying the impact of environmental change on past rates of carbon accumulation (Ratcliffe & Payne 2016). Major changes have occurred across the Scottish peatland landscape at various points throughout the Holocene, for example the temporary expansion of *Pinus sylvestris* across previously treeless peatland (Gear & Huntley 1991), and the sudden decline and regional extinction of species which were previously widespread, such as *Sphagnum austinii* (formerly known as *Sphagnum imbricatum*) (Hughes *et al.* 2008, McClymont *et al.* 2008). Despite a well-studied palaeoecology, long-term carbon accumulation data for Scotland, and for oceanic peatlands in general, is lacking (Lindsay 2010, Loisel & Yu 2013, Payne *et al.* 2016, Chaudhary *et al.* 2017, Ratcliffe *et al.* 2018). Oceanic is defined here as occurring within the fully humid warm temperate climatic zone, i.e. Cf as defined in the updated Köppen-Geiger climate classification (Kottek *et al.* 2006).

Globally, several large compilations of long-term carbon accumulation data have been produced (e.g. Vitt *et al.* 2000, Yu *et al.* 2009, 2010; van Bellen *et al.* 2011, Charman *et al.* 2013, Loisel & Yu 2013). However the drivers of long-term carbon dynamics appear inconsistent across peatland types and regions (Loisel & Yu 2013, van der Linden *et al.* 2014, Charman *et al.* 2015), with concerns that oceanic peatlands, under-represented in past compilations, may not respond to climate in the same way as their continental counterparts. For example, cooler winters are more likely to reduce plant productivity in oceanic climates, where winter growth may usually occur (Loisel & Yu 2013). Observed data for Scotland (e.g. Anderson 2002) do not appear to fit global models of peat-carbon-climate, implying that different controls might apply in these sites (Chaudhary *et al.* 2017), and significant gaps in our understanding of the drivers of long-term C accumulation remain (Magnan & Garneau 2014). Here we focus our attention on the largest area of oceanic blanket bog in the UK: the Flow Country of Caithness and Sutherland (Warren 2000).

We use a total of 55 records, comprised of nine new carbon accumulation records, three re-analysed records and 43 additional age-depth models to infer changes in carbon accumulation through the Holocene. We then place these data in the context of 'known' Scottish palaeoclimatic changes and compare these with other global records.

## METHODS

### Site description

The Flow Country of Caithness and Sutherland (Figure 1) covers an area of 400,000 ha (Lindsay *et al.* 1988) of almost continuous deep peatland bounded by the coast to the north, the river Thurso in the east, the settlement of Kinbrace in the south, and the Strath of Naver to the west (Lindsay *et al.* 1988), and extends much farther south and west than this in a less continuous form (Charman 1990). For the purposes of this study we defined the Flow Country as all of mainland Scotland north of 57.85 °N, equivalent to an east–west line between the town of Ullapool and the Dornoch Firth. The climate of this region is classed as hyperoceanic and very humid (Birse 1971) and is generally wetter in the west. Forsinard, in the centre of the Flow Country, receives on average 1020 mm of rain spread over 200 days (Met Office 2014a). Mean daily temperatures tend to be around 8 °C on the coast, decreasing to between 7.5 and 6 °C for the central Flow Country (Met Office 2014b).

### New and re-analysed carbon accumulation reconstructions

Here we present 12 records of carbon accumulation from Flow Country peatlands. Three of these have been published previously (Ratcliffe *et al.* 2018), two are entirely new, and a further five have been presented only in unpublished theses (Ratcliffe 2015, B.A.V. Smith 2016). While there is some variation in methodology, we identify the key approaches which are common to all records and state how they differ for individual cases.

### Field sites

Twelve cores were taken from five sites located across the Flow Country, with the east of the region best represented (Figure 1). Six of the cores were from areas of bog that were in a near-natural state, i.e. there was little or no evidence of recent disturbance; while five of the cores were from areas planted for forestry. One core, GB2, was from a site where peat cutting is known to occur.

Informed interpretation is required in consideration of the forested and cut sites; for instance, disturbance and possible loss of carbon may


 DOI: 10.19189/MaP.2018.OMB.347

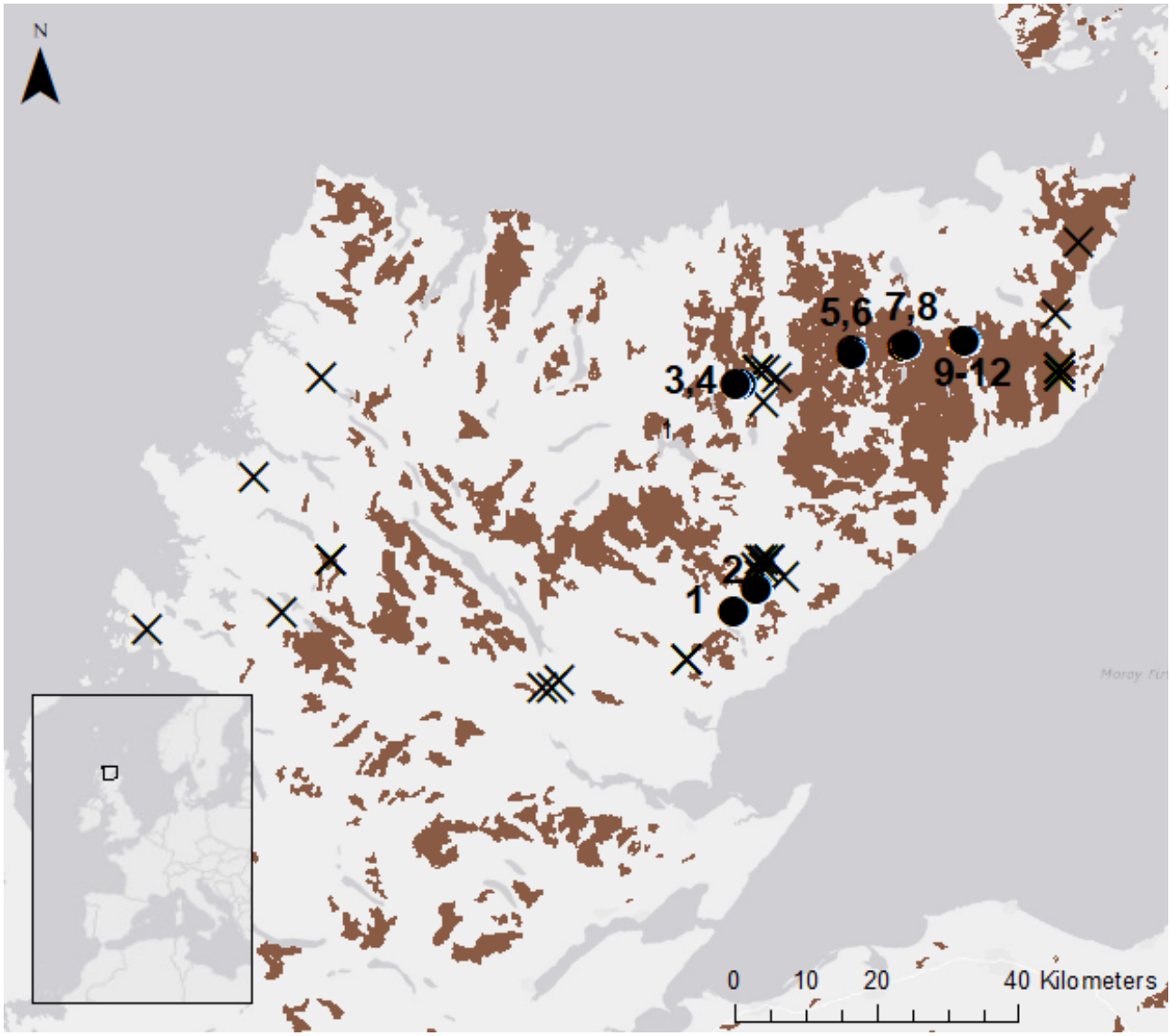


Figure 1. Sites for which carbon accumulation has been inferred (crosses) and measured (circles). Brown shading indicates areas of deep peat from the James Hutton Institute peat map (Scottish Government 2018). Numbers indicate the measured sites: 1) GB1, 2) GB2, 3) CRSLF, 4) CRSLO, 5) CATO, 6) CATF, 7) BRAEO, 8) BRAEF, 9) BADO, 10) BADF, 11) BADP1 and 12) BADP2.

have occurred in the upper peat layers. These sites represent carbon accumulation in the minority of the Flow Country which has been disturbed by human activity, for example the estimated 17 % of Flow Country peatlands which are planted with coniferous forest (Lindsay *et al.* 1988). However, it is important to recognise that these sites do not reflect carbon accumulation in near-natural sites and we have, therefore, presented statistics calculated both from the total dataset and when excluding these records. Below we provide a brief description of the individual sites from which the records were obtained.

**Bad a' Cheo** is an area of blanket bog located at the eastern edge of the Flow Country at approximately 95 metres above sea level (m a.s.l.). BADO and BADP1 were from near-natural parts of the site with well-developed microtopography (hummocks, hollows and pools). Vegetation was dominated by *Sphagnum*, the most abundant species being *Sphagnum magellanicum* and *Sphagnum papillosum* (Lindsay *et al.* 1988). BADF and BADP2 were from an area of coniferous forest plantation with incomplete ground vegetation cover, an extensive carpet of needle litter, and microtopography primarily reflecting disturbance during afforestation.


 DOI: 10.19189/MaP.2018.OMB.347

**Catanach** is located farther west, near the Altnabreac railway station, in an area with continuous peat at approximately 200 m a.s.l. The climate at Catanach is believed to be more humid than at other sites discussed here due to the influence of the Knockfin Heights to the south (Lindsay *et al.* 1988). CATO was an open site on a slope to the north-west with vegetation described as *Sphagnum* - *Betula nana* - *Arctostaphylos uva-ursi* mire by Lindsay *et al.* (1988). CATF was located on sloping terrain to the south with conifer plantation and limited brown moss dominated understorey vegetation.

**Braehour** is at 130 m a.s.l. with peat depth varying between 6.5 and 1.3 metres (Ratcliffe & Payne 2016). The dominant plant cover of the open site (BRAEO) was *Eriophorum vaginatum* growing within a matrix *of Sphagnum* spp. The area is notable for the numerous archaeological remains nearby, which provide evidence of human settlement and agricultural activity (Peteranna 2012). BRAEF was nearby within a plantation of *Pinus contorta*.

**Cross Lochs** is one of the more intensively studied regions of the Flow Country and is located at 230 m a.s.l. Peat depth varies between 0.64 and 4.00 metres (Ratcliffe & Payne 2016, Holden *et al.* 2017). Cross Lochs is a mixture of ombrotrophic blanket bog and ladder fen (Charman 1994). CRSLO was taken from a gently sloping area of ombrotrophic bog dominated by *Sphagnum* spp. (including *S. cuspidatum*, *S. papillosum* and *S. fallax)* in addition to *Calluna vulgaris*, *Trichophorum germanicum* and *Eriophorum angustifolium*. CRSLF was taken from an area which had been planted with *Pinus contorta* and *Picea sitchensis* for commercial forestry.

**Gordonbush** is the most southerly site investigated, located approximately 10 km from the town of Brora. GB1 was located on blanket bog at 370 m a.s.l. on a south-west facing hillslope, the highest of our sites. GB2 was located at 170 m a.s.l. on the saddle between two small hills where historical peat cutting is known to have occurred. Indeed, the core was taken from a depression with morphology suggesting this area had been cut. Vegetation at both sites included *Eriophorum* spp., *C. vulgaris* and *Sphagnum* spp. (B.A.V. Smith 2016).

**Coring method**

Peat cores were retrieved from all sites using a Russian corer (Belokoptyov & Beresnevich 1955 in Jowsey 1966). Sampling was carried out from the midpoint between hummock and hollow microforms, when they were apparent, down to the mineral substrate. Cores taken from the near-natural locations (see Table 4) were considered representative of the local vegetation. Coring for the forested sites (Table 4) was carried out on the original surface to minimise the chance of disturbance in the upper peat layers as a result of ploughing. The twin borehole method was used with a minimum of 5 cm overlaps in order to minimise the risk of core compression, as outlined by De Vleeschouwer *et al.* (2010).

**Bulk density**

Bulk density measurements were carried out continually down each core, at increments of 1 cm (CRSLO), 2 cm (BADP1, BADP2) or 5 cm (CATO, CATF, CRSLF, BRAEO, BADO, BADF, BRAEF). Sample volume was determined using the water displacement technique (Chambers *et al.* 2011), as described in Ratcliffe *et al*. (2018). Wet peat samples approximately 10–20 $cm^3$ in size were carefully removed from the cores and placed into a volumetric cylinder where water volume displaced was recorded. Samples were then dried at 105 °C and weighed. Raw Data for GB1 and GB2 were unavailable, and were instead obtained from plots in B.A.V. Smith (2016) using the software Digitalizer (Mitchell *et al.* 2017).

**C content**

Carbon content of dry peat was measured for CRSLO, CRSLF, CATF, CATO, BRAEO, BRAEF, BADO and BADF using an elemental analyser (Carlo Erba 1108 at University of Stirling), which was calibrated for each run using rice flour standards with standard checks every 10–12 samples (Ratcliffe *et al.* 2018). For BADP1 and BADP2 a different elemental analyser was used (Elementar Vario Macro at University of York), where glutamic acid standards were used for calibration with standard checks every 12 runs. The carbon content for GB1 and GB2 was estimated from ash free bulk density and an assumed carbon content of 50 % for the organic matter lost, based on the literature for *Sphagnum* peat (Beilman *et al.* 2009). Ash free bulk density was calculated by deducting the weight of the mineral faction from dry bulk density, with the weight of the mineral faction determined by combusting the samples in a muffle furnace at 550 °C for four hours.

**C accumulation**

A combination of radiocarbon and cryptotephra derived dates were used to construct age-depth models to provide a timescale over which the carbon measured down-core had accumulated. A total of 32 radiocarbon dates were derived from AMS radiocarbon samples. Thirteen of these dates have been published previously in Ratcliffe *et al.* (2018)


 DOI: 10.19189/MaP.2018.OMB.347

and details of the remaining 19 are provided in Table 1. Individual above-ground macrofossils were dated when possible but bulk samples were also dated for some highly humified peats. Recent research has shown no systematic offset between bulk and surface macrofossil dates (Holmquist *et al.* 2016); therefore, we anticipated no systemic bias to have resulted from combining the two methods.

For a subset of cores (Table 2) dates derived from cryptotephra (volcanic ash not visible to the naked eye) were used to support radiocarbon chronologies. Cryptotephra were located using a combination of microscopy, loss on ignition analysis, xradiography and XRF core scanning (Ratcliffe *et al.* 2018). Shards from identified layers were geochemically analysed using a Cemeca SX100 electron probe microanalyser (EPMA) at the School of GeoSciences, University of Edinburgh. Operating conditions were: an accelerating voltage of 15 kV, a beam current of 2 nA (Na, Mg, Al, Si, Ca, Fe, and K) and 80 nA (Ti, Mn and P), and a beam diameter of 5 μm. Reference geochemical data was obtained from Tephrabase (Newton *et al.* 2007) and used to identify sources of the tephras located. Based on the recommendations in Dugmore *et al*. (1995), distinctive oxide ratios of FeO and $TiO_2$ were primarily used in the identification of Hekla 4 (Figure A1 in the Appendix) and Lairg A (Figure A2). Results for CRSLO, CATO and BADO were previously published in Ratcliffe *et al*. (2018); here we focus on results for three further cores, BADF, CRSLF and CATF. Once cryptotephra layers had been linked to a known eruption, ages and uncertainty were assigned to the cryptotephra layers following the compilation of Swindles *et al*. (2011).

Table 1. Full details of radiocarbon dates for cores not previously published. Calibrated ages were derived from the BACON age-depth models with the INTCAL13 calibration curve. Best estimate of the calibrated date is presented as the weighted mean following the recommendation of Telford *et al*. (2004).

| Core: | Lab no. | Mid-point depth (cm) | Material selected for dating | Radiocarbon date(BP) | Best estimate (cal BP) | 95 % confidence range (cal BP) |
|---|---|---|---|---|---|---|
| CRSLF | Poz-62865 | 185 | charcoal | 5090 ± 40 | 5851 | 5591–6038 |
| BADF | D-AMS 006129 | 353 | *Betula* stem | 8855 ± 31 | 9938 | 9690–10166 |
| BRAEF | D-AMS 006123 | 131.5 | bulk peat | 2516 ± 23 | 2587 | 2366–2773 |
| BRAEO | D-AMS 006124 | 134.5 | bulk peat | 4198 ± 33 | 4881 | 4679–5113 |
| GB1 | SUERC-46754 | 25.5 | bulk peat | 1048 ± 29 | 954 | 810–1060 |
| GB1 | SUERC-42928 | 57.5 | bulk peat | 1739 ± 25 | 1671 | 1569–1809 |
| GB1 | SUERC-49279 | 75.5 | bulk peat | 2328 ± 29 | 2309 | 2132–2455 |
| GB1 | SUERC-42927 | 149.5 | bulk peat | 3598 ± 29 | 3918 | 3760-4063 |
| GB1 | SUERC-49283 | 175.5 | bulk peat | 4001 ± 30 | 4486 | 4333–4625 |
| GB1 | SUERC-46756 | 199.5 | bulk peat | 4438 ± 27 | 5096 | 4873–5304 |
| GB1 | SUERC-42929 | 285.5 | bulk peat | 7931 ± 30 | 6585 | 5926–7291 |
| GB2 | SUREC-46757 | 27.5 | bulk peat | 1464 ± 26 | 1350 | 1267–1474 |
| GB2 | SUERC-42930 | 57.5 | bulk peat | 2640 ± 29 | 2698 | 2340–2890 |
| GB2 | SUERC-46758 | 99.5 | bulk peat | 3354 ± 29 | 3634 | 3502–3804 |
| GB2 | SUERC-42931 | 134.5 | bulk peat | 4144 ± 24 | 4668 | 4523–4832 |
| GB2 | SUERC-46759 | 200.5 | bulk peat | 4973 ± 29 | 5783 | 5603–5945 |
| GB2 | SUERC-42932 | 261.5 | bulk peat | 7640 ± 30 | 8356 | 7986–8576 |
| BADP1 | D-AMS 024944 | 526 | bulk peat | 9118 ± 52 | 10308 | 10012–10555 |
| BADP2 | D-AMS 024945 | 415 | bulk peat | 8899 ± 49 | 9962 | 9577–10244 |


 DOI: 10.19189/MaP.2018.OMB.347

Age-depth models (Figure A3) were constructed in the Bayesian modelling package BACON (Blaauw & Christen 2011). BACON uses prior information such as plausible accumulation rates and the law of superposition to reduce uncertainty and produce a more realistic model (Blaauw & Christen 2011). The prior for accumulation rate was set at 10 cm $yr^{-1}$, a 5 cm section depth was specified and other accumulation and memory priors were left at the default values following Goring *et al*. (2012). A suspected hiatus in peat accumulation was specified for GB2 at 60 cm in line with the estimated peat cutting depth identified in B.A.V. Smith (2016).

The carbon density of each segment, corresponding to the sub-sampling interval for bulk density and carbon content, was calculated from the bulk density of peat multiplied by the carbon content of the dry organic matter. Carbon density was then divided by the difference between the modelled age of the base and top of each segment, or the time taken for the carbon in the segment to accumulate, to produce annual carbon accumulation reconstructions.

**Inferred carbon accumulation simulations**

Although our data collection means there are now more carbon accumulation records for the Flow Country than for any other equivalently-sized area of UK peatland, these are still few in number relative to the area of peat and the variability in peatland habitat. There are many more sites in the region which have been previously cored for palaeoecological study but where carbon content and bulk density have not been analysed. These inferred records give information on peat accumulation rates for a much larger range of sites. As peat accumulation rate is one of the most variable terms in the carbon accumulation calculation, these sites can also give information on variability in carbon accumulation rates to support our primary carbon accumulation records. We conducted a meta-analysis of these peat accumulation records and used information on carbon content taken from locations where this was available to model plausible patterns of carbon accumulation for this larger group of sites; a schematic diagram of this process is provided in Figure A4.

We first compiled published dating information for Flow Country peat records. We identified all radiocarbon dated peat cores from this region based primarily on the database of Payne *et al*. (2016) and identified cores where full radiocarbon details were presented. We did not include sites solely with dates based on methods other than radiocarbon (e.g. sites with just a tephra layer) or coastal sites, as per the methodology of Payne *et al*. (2016). Only dates for peat were included in the analysis, with any dates on non-peat sediment excluded. Based on these criteria we identified 43 sites with useful data (Table 3), including 126 individual dates. We extracted dating information from the original publications, re-calibrated dates to the IntCal13 calibration curve (Reimer *et al.* 2013), and produced new age-depth models using BACON with parameterisation as above. The surface was included as a dating point and assigned to the year of publication of the study as actual year of sampling was frequently not stated. Using the weighted mean of the BACON runs we calculated peat accumulation rates for each 500-year period from 0 to 10,500 cal BP.

Table 2. Identified tephra layers which could be linked to previously-described tephra based on their major element geochemistry. Reference data for identification were taken from Tephrabase (Newton *et al.* 2007). The tephra layers found are generally referred to by the site code and depth; for example, BADO 200 indicates the tephra located at 200 cm depth in core BADO. * indicates tephra for which geochemical data are available in Ratcliffe *et al*. (2018).

| Depth (cm) | BADO | BADF | CATO | CATF | CRSLO | CRSLF | BRAEO |
|---|---|---|---|---|---|---|---|
| 97.4 | | | | Hekla 4 | | | |
| 102.4 | | | | | | | Hekla 4 |
| 114.4 | | Hekla 4 | | | | | |
| 116.7 | | | Hekla 4* | | | | |
| 122.7 | | | | | | Hekla 4 | |
| 134.3 | Glen Garry* | | | | | | |
| 165.6 | | | | | Hekla 4* | | |
| 200.1 | Hekla 4* | | | | | | |
| 228 | | Lairg A | | | | | |


 DOI: 10.19189/MaP.2018.OMB.347

Table 3. Details of radiocarbon dated peat core records used in this study listing core name (as defined in original study), location (UK Ordnance Survey coordinates), number of dates, age of oldest date on peat (uncalibrated $^{14}$C years BP) and original reference with * indicating an unpublished thesis. Core locations are based on original coordinates or our interpretations of information provided in the original reference. Note that some cores are discussed in more than one reference; we make no attempt to identify all relevant publications.

| Core | Location | Number of dates | Oldest date (BP) | Reference |
|---|---|---|---|---|
| Aukhorn | ND326636 | 4 | 7895 | Robinson (1987) |
| Badentarbet | NC011098 | 6 | 3890 | Bunting & Tipping (2004) |
| Craggie Basin- 1 | NC872184 | 1 | 4150 | Mills *et al*. in Gallego-Sala *et al*. (2015) |
| Craggie Basin- 11 | NC874175 | 1 | 5370 | Mills *et al*. in Gallego-Sala *et al*. (2015) |
| Craggie Basin- 15 | NC883186 | 1 | 3600 | Mills *et al*. in Gallego-Sala *et al*. (2015) |
| Craggie Basin- 19 | NC885190 | 1 | 2860 | Mills *et al*. in Gallego-Sala *et al*. (2015) |
| Craggie Basin- 23 | NC888197 | 1 | 2630 | Mills *et al*. in Gallego-Sala *et al*. (2015) |
| Craggie Basin- 29 | NC891193 | 1 | 8800 | Mills *et al*. in Gallego-Sala *et al*. (2015) |
| Craggie Basin- 34 | NC890192 | 1 | 1730 | Mills *et al*. in Gallego-Sala *et al*. (2015) |
| Craggie Basin- 37 | NC909168 | 1 | 4320 | Mills *et al*. in Gallego-Sala *et al*. (2015) |
| Craggie Basin- 6 | NC875200 | 1 | 4650 | Mills *et al*. in Gallego-Sala *et al*. (2015) |
| Cross Lochs- CLA1 | NC883460 | 6 | 8995 | Charman (1990) * |
| Cross Lochs- Monolith 1 | NC87 46 | 1 | 9170 | Charman (1990) * |
| Cross Lochs- Monolith 2 | NC87 46 | 3 | 4890 | Charman (1990) * |
| Cross Lochs- Monolith 3 | NC87 46 | 3 | 6805 | Charman (1990) * |
| Cross Lochs- Monolith 4 | NC87 46 | 1 | 8835 | Charman (1990) * |
| Forsinard (Coulson) | NC900450 | 1 | 4560 | Coulson *et al*. (2005) |
| Forsinard (Tallis) | NC885412 | 3 | 3052 | J. Tallis (unpublished) |
| Lairg- AG1 | NC592023 | 11 | 8460 | M.A. Smith (1996) * |
| Lairg- AG2 | NC567013 | 12 | 8470 | M.A. Smith (1996) * |
| Lairg- AG3 | NC583018 | 14 | 6970 | M.A. Smith (1996) * |
| Loch Farlary- A13 | NC773049 | 2 | 6605 | Tipping *et al*. (2007a) |
| Loch Farlary- L19 | NC773049 | 1 | 7860 | Tipping *et al*. (2007a) |
| Loch Farlary- Y25 | NC773049 | 7 | 10570 | Tipping *et al*. (2007a) |
| Loch Laxford | NC259454 | 5 | 1395 | Stefanova *et al*. (2008) |
| Loch of Winless | ND295545 | 7 | 8650 | Peglar (1979) |
| Loch Veyatie | NC200120 | 2 | 3300 | Davies (2011) |
| Oliclett- 250E 190N | ND302465 | 1 | 2140 | Tipping *et al*. (2007b) |
| Oliclett- 260E 150N | ND302453 | 1 | 7660 | Tipping *et al*. (2007b) |
| Oliclett- 260E 180N | ND302454 | 1 | 6170 | Tipping *et al*. (2007b) |
| Oliclett- 260E 200N | ND302456 | 1 | 1535 | Tipping *et al*. (2007b) |
| Oliclett- 264E 200N | ND302457 | 1 | 6200 | Tipping *et al*. (2007b) |
| Oliclett- 265E 190N | ND302455 | 1 | 5275 | Tipping *et al*. (2007b) |
| Oliclett- 315E 220N | ND302462 | 1 | 3420 | Tipping *et al*. (2007b) |
| Oliclett- 335E 220N | ND302461 | 1 | 3420 | Tipping *et al*. (2007b) |
| Oliclett- 375E 150N | ND302464 | 1 | 2910 | Tipping *et al*. (2007b) |
| Oliclett- 400E 150N | ND302463 | 1 | 3265 | Tipping *et al*. (2007b) |
| Oliclett- 400E 220N | ND302460 | 1 | 3480 | Tipping *et al*. (2007b) |
| Oliclett- 450E 150N | ND302458 | 1 | 4255 | Tipping *et al*. (2007b) |
| Ruigh Dorch | NC161307 | 2 | 4730 | Davies (2011) |
| Traligill Basin- 1 | NC27 20 | 5 | 2705 | Charman *et al*. (2001) |
| Traligill Basin- 2 | NC27 20 | 4 | 2325 | Charman *et al*. (2001) |
| Traligill Basin- 4 | NC27 20 | 5 | 2165 | Charman *et al*. (2001) |


 DOI: 10.19189/MaP.2018.OMB.347

There were large differences in the quality of the chronologies between the individual studies, with the number of radiocarbon dates per core varying from one to 14 and several cores represented by a single basal date. This resulted in considerable variability in the precision of the age-depth models for any given period. To avoid giving undue weight to imprecise models based on sparse dating, we weighted results by model precision. For the centre point of each 500 year bin we calculated prediction range for each BACON model, standardised these data as z-scores, and used to weight mean accumulation rates by age-depth model precision. We present accumulation rates both as raw, unweighted means for each 500 year bin and as means weighted by model precision.

The data for these 43 sites did not include information on bulk density and carbon content of the peat. However, as peat accumulation rate is an important determinant of carbon accumulation, we used the data to infer potential carbon accumulation trajectories. We made two simplifying assumptions: i) that sites with bulk density and carbon data are representative of the larger number of sites with age-depth models only; and ii) that temporal change in peat carbon density is spatially coherent across the study region. For each 500-year bin in each site-specific age-depth model we randomly assigned a carbon density value (i.e. carbon content of dry peat multiplied by bulk density) derived from one sample in the appropriate time period from one of the 12 sites with such data. We repeated this process through 1000 cycles of random re-sampling to estimate mean carbon accumulation rate for each bin in each site, and then summed across sites to estimate mean carbon accumulation rates. Finally, we weighted the results by age-depth model precision, as above. The resulting inferred carbon accumulation curves provide a means to evaluate plausible carbon accumulation trajectories in a wider range of sites.

## RESULTS

### New and re-analysed carbon accumulation records

*Chronology*

Radiocarbon and tephra dates revealed peat initiation ages ranging from 2516 cal BP at BRAEF to 10308 cal BP at BADP1. A total of nine cryptotephra layers were found, from thee unique eruptions. Upon geochemical analysis it was evident that seven of these matched the geochemistry of the Hekla 4 tephra (Figure A1 in the Appendix), which was located in seven cores (Table 2). The remaining two tephra layers from other eruptions were found in one core each. These were identified as Glen Garry (data shown in Ratcliffe *et al*. 2018) at 134.3 cm in the BADO core, and Lairg A (Figure A2) at 228.0 cm in BADF (Table 2). It is of note that shards from Lairg A, in measurable quantities, have previously been found only at two sites in Scotland, namely Lairg (Dugmore *et al.* 1995) and Temple Hill Moss (Langdon *et al.* 2003), with Bad a' Cheo now representing the northernmost site in Scotland.

*Physical properties*

The average bulk density for the sites was 0.088 ± 0.020 g $cm^{-3}$ and the lowest mean bulk densities were seen in BADO, BADP1, GB1 and GB2. All records had relatively low and consistent values between 0.065 and 0.068 g $cm^{-3}$. The highest mean bulk density was for the BRAEF core (from forested peat) and was 0.120 g $cm^{-3}$. The forested cores had consistently higher bulk density than the near natural sites (Table 4). Individual records (Ratcliffe 2015, B.A.V. Smith 2016) displayed a consistent trend of declining bulk density down-core from the surface, reaching a minimum between 20 and 80 cm depth, whereupon bulk density began to climb again towards the base of the core. On average, the mean carbon content of the dry peat was 52.9 % and was found to increase with depth across all sites, with values around 45 % common for the surface peat and values greater than 60 % for some of the basal peats at Catanach and Bad a' Cheo.

*Carbon accumulation*

We present the carbon accumulation data as a time weighted average for the cores. We focus on results below 50 cm depth (ranging from 830 to 2300 cal BP in age), with 50 cm being a plausible upper boundary for acrotelm thickness (Clymo 1984) which is unlikely to be exceeded in our sites. The reason for excluding acrotelm peats is that they are relatively undecomposed and carbon accumulation data for this zone will give high apparent rates which are not directly comparable with carbon accumulation values from the deeper catotelm, and indeed the two are often poorly correlated (Turunen 2003). With the top 50 cm excluded we calculated a time weighted mean carbon accumulation rate of 17.8 g $m^{-2}$ $year^{-1}$ for all sites (Table 5); this was 17.9 g $m^{-2}$ $year^{-1}$ for near natural sites and 17.7 g $m^{-2}$ $year^{-1}$ for forested and cut sites. If the top 50 cm are included in the estimate, this changes to 17.2, 16.7 and 17.9 g $m^{-2}$ $year^{-1}$ for all, near natural, and forested and cut sites, respectively. For comparability with other studies, we also calculated the long-term apparent rate of C


 DOI: 10.19189/MaP.2018.OMB.347

Table 4: New and re-analysed records of carbon accumulation including the location of the core, the number of dating points used (radiocarbon and tephra derived), the oldest date available (uncalibrated radiocarbon years), the disturbance status of the site (where near natural indicates no visible signs of disturbance), and the primary reference (where previously published). * indicates a calibrated age in BP, derived from the Hekla 4 eruption.

| Site | Record | Location | Dates | Oldest date (BP) | Status | Primary source |
|---|---|---|---|---|---|---|
| Bad a' Cheo | BADO | ND 16500 50174 | 3 | 7830 | near natural | Ratcliffe *et al*. (2018) |
| Bad a' Cheo | BADF | ND 16705 50158 | 3 | 8855 | forested | Ratcliffe (2015) |
| Catanach | CATO | ND 00605 48769 | 2 | 5080 | near natural | Ratcliffe *et al*. (2018) |
| Catanach | CATF | ND 00533 48289 | 1 | 4287* | forested | Ratcliffe (2015) |
| Braehour | BRAEO | ND 07892 49381 | 2 | 4198 | near natural | Ratcliffe (2015) |
| Braehour | BRAEF | ND 08208 49512 | 1 | 2516 | forested | Ratcliffe (2015) |
| Cross Lochs | CRSLO | NC 85095 44154 | 12 | 8567 | near natural | Ratcliffe *et al*. (2018) |
| Cross Lochs | CRSLF | NC 84134 43941 | 2 | 5090 | forested | Ratcliffe (2015) |
| Gordonbush | GB1 | NC 87049 15176 | 7 | 7931 | near natural | B.A.V. Smith (2016) |
| Gordonbush | GB2 | NC 83945 12078 | 6 | 7640 | cut | B.A.V. Smith (2016) |
| Bad a' Cheo | BADP1 | ND 16314 50168 | 1 | 9118 | near natural | unpublished |
| Bad a' Cheo | BADP2 | ND 16601 49921 | 1 | 8899 | forested | unpublished |

Table 5. Summary data for new and re-analysed records. The values reported are means ± standard deviation. Standard deviations were derived using the values for every segment in each core. Summarised data are provided for bulk density, % C content of dry peat, total C accumulated from the base of the peat to the surface, the long-term apparent rate of C accumulation (LARCA) which is provided for comparability purposes, and the time weighted C accumulation which excludes the upper 50 cm to avoid inclusion of undecomposed acrotelm peat.

| Record | Mean bulk density in ($g\ cm^{-3}$) | % C content of dry peat | Total C ($kg\ m^{-2}$) | LARCA ($g\ m^{-2}\ year^{-1}$) | Time weighted C accumulation, excluding top 50 cm ($g\ m^{-2}\ year^{-1}$) |
|---|---|---|---|---|---|
| BADO | 0.067 ± 0.010 | 52.3 ± 4.1 | 147.9 ± 0.3 | 17.2 | 17.7 ± 4.8 |
| BADF | 0.094 ± 0.024 | 51.2 ± 5.0 | 168.4 ± 0.6 | 17.0 | 17.4 ± 3.9 |
| BADP1 | 0.065 ± 0.019 | 54.6 ± 6.1 | 185.0 ± 0.6 | 18.0 | 19.4 ± 5.6 |
| BADP2 | 0.080 ± 0.020 | 54.8 ± 3.3 | 177.3 ± 0.5 | 17.8 | 17.7 ± 2.6 |
| BRAEO | 0.119 ± 0.019 | 50.0 ± 2.7 | 76.1 ± 0.6 | 15.6 | 24.1 ± 13.6 |
| BRAEF | 0.120 ± 0.015 | 50.4 ± 3.7 | 77.0 ± 0.4 | 29.8 | 29.5 ± 5.2 |
| CATO | 0.107 ± 0.024 | 58.0 ± 4.3 | 95.7 ± 0.6 | 16.4 | 16.5 ± 2.9 |
| CATF | 0.111 ± 0.018 | 51.1 ± 2.6 | 52.4 ±0.4 | 12.2 | 12.0 ± 1.0 |
| CRSLO | 0.082 ± 0.013 | 52.0 ± 2.4 | 145.9 ± 0.1 | 15.3 | 18.1 ± 4.8 |
| CRSLF | 0.090 ± 0.026 | 54.4 ± 2.9 | 88.8 ± 0.6 | 15.2 | 15.4 ± 4.4 |
| GB1 | 0.065 ± 0.017 | N/A | 93.0 ± 0.3 | 10.7 | 11.4 ± 2.5 |
| GB2 | 0.068 ± 0.014 | N/A | 88.2 ± 0.3 | 10.5 | 14.2 ± 6.0 |
| mean | 0.088 ± 0.020 | 52.9 ± 2.5 | 116.3 ± 45.5 | 16.3 ± 5.0 | 17.8 ± 4.9 |


 DOI: 10.19189/MaP.2018.OMB.347

accumulation (LARCA), by simply dividing the total C in each core by the calibrated age of the deepest point. This produced rates of 16.3 g $m^{-2}$ $year^{-1}$ for all sites (Table 5), 15.5 g $m^{-2}$ $year^{-1}$ for near natural and 17.1 g $m^{-2}$ $year^{-1}$ for forested and cut sites. It should be noted that these estimates of LARCA include the top 50 cm.

The greatest carbon accumulation rate was seen in BRAEO (46.8 g $m^{-2}$ $year^{-1}$ at 4800 cal BP), while the lowest was seen in GB2 (4.8 at 600 cal BP). All records displayed a minimum for carbon accumulation in the mid-to-late Holocene, between 6000 and 500 cal BP (Figure 2), though the exact timing varied greatly between sites. The maximum rates of carbon accumulation, excluding the surface peat, often occurred in the first millennium after initiation, but there were multiple exceptions to this. For example, GB1, GB2, BADF and CRSLO all displayed maximum rates of carbon accumulation several thousand years after initiation. Peat formation occurred first at Bad a' Cheo, CRSLO and Gordonbush initiated between 8380 and 10308 cal BP, followed by a general pattern of high early Holocene carbon accumulation which began to decline from 8000 cal BP onwards (Figure 2). At ~ 5850 cal BP peat initiated at CATO and CRSLF and all sites continued to display declining carbon accumulation until ~ 5000 cal BP, with the exception of GB2 where carbon accumulation approximately tripled from ~ 8 g $m^{-2}$ $year^{-1}$ to ~ 24 g $m^{-2}$ $year^{-1}$ at 5700 cal BP. Around this time peat formation initiated at BRAEO (4881 cal BP) and CATF (4280 cal BP). From this period onwards, carbon accumulation records differ more across sites, with some such as BADO and BADF undergoing a sharper decline in carbon accumulation than previously seen (decline of >10 g $m^{-2}$ $year^{-1}$), while others such as CRSLO and GB2 showed a near synchronous and similarly sharp increase in C accumulation (increase of >10 g $m^{-2}$ $year^{-1}$). Other records including BRAEO, BADP1, BADP2, GB1 and CATO displayed either gradually declining carbon accumulation or steady values. There are similar contrasting responses across records around 2500 cal BP, with BADO, BADF and CRSLF displaying an increase in carbon accumulation (increase of >5 g $m^{-2}$ $year^{-1}$) and CRSLO and GB2 showing declining carbon accumulation (decline of >3 g $m^{-2}$ $year^{-1}$). The period from 2000 cal BP onwards is not discussed, as it is represented by peat shallower than 50 cm for several records. This lies outside our conservative estimate of what constitutes catotelm peat, and thus is not easily comparable to earlier periods of carbon sequestration.

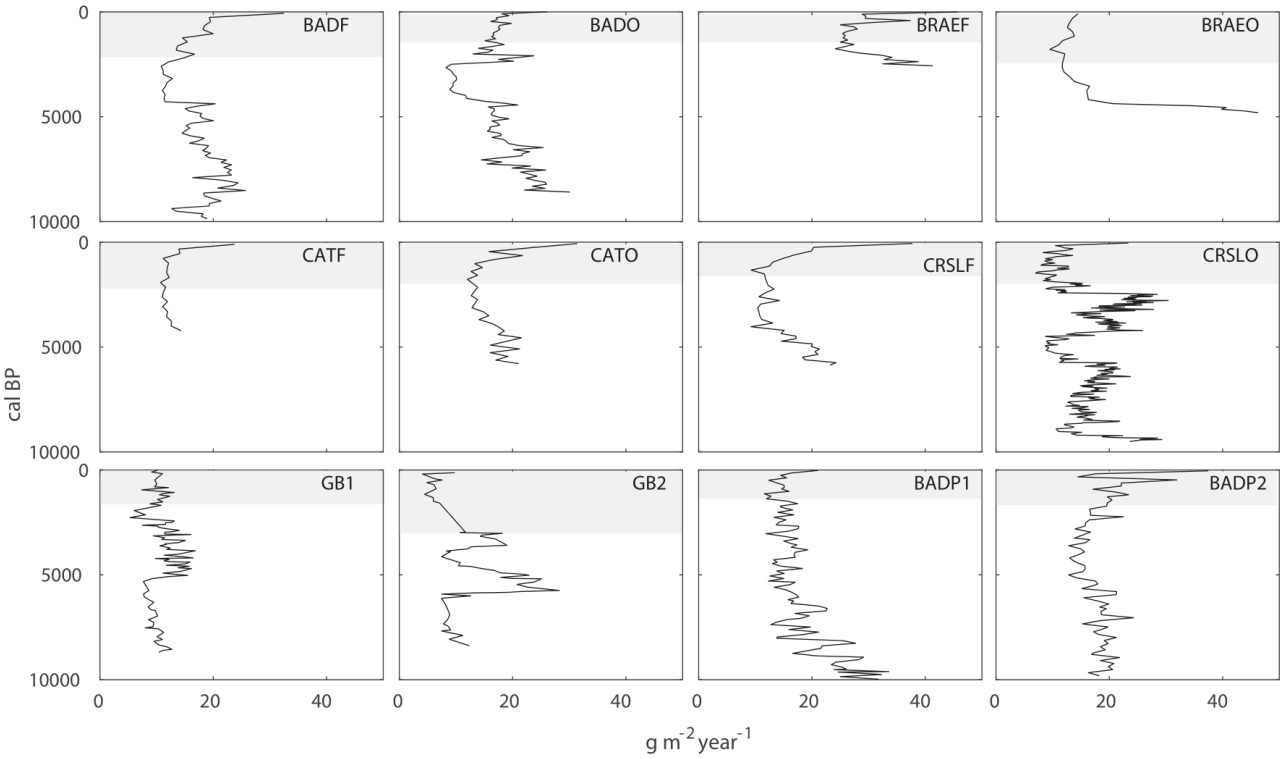


Figure 2. New and re-analysed records of carbon accumulation for the Flow Country. Area shaded in grey represents the upper 50 cm of the core and the transition to acrotelm peat. CRSLO, CATO and BADO have been previously published in Ratcliffe *et al*. (2018).


 DOI: 10.19189/MaP.2018.OMB.347

**Inferred rates of carbon accumulation**

Across the 43 peatlands with published dating information, the site average peat accumulation rate (Figure 3) was 0.033 ± 0.015 cm $yr^{-1}$. This was initially high (0.035–0.047 cm $yr^{-1}$) before 8000 cal BP and gradually fell to 0.030–0.035 cm $yr^{-1}$ between 2000 and 5000 cal BP, with the lowest rate of peat accumulation (0.022 cm $yr^{-1}$) occurring at 4500 cal BP. Peat accumulation started to increase from 4000 cal BP onwards, and peaked near the surface as the undecomposed acrotelm peat is reached.

Inferred carbon accumulation rates based on these age-depth models varied between 23 and 12 g $m^{-2}$ $yr^{-1}$ (Figure 3), with highest rates (> 20 g $m^{-2}$ $yr^{-1}$) occurring in the early Holocene (8000–9000 cal BP). From this early peak, values declined sharply to 14 g $m^{-2}$ $yr^{-1}$ then plateaued from 7500 to 4500 cal BP. A small increase in C accumulation rate to 16 g $m^{-2}$ $yr^{-1}$ occurred around 4000 cal BP and was subsequently followed by a drop to the lowest rate

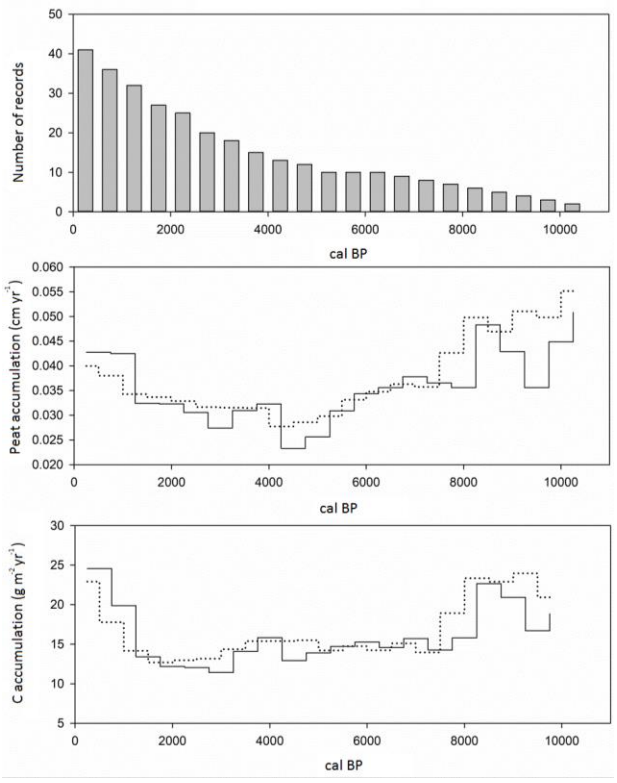


Figure 3. Peat and carbon accumulation, inferred from sites with age-depth models only. The plots show number of sites contributing (grey bars, top plot), unweighted (dotted) and weighted peat accumulation (black line, middle plot) and unweighted (dotted, bottom plot) and weighted (black, bottom plot) inferred carbon accumulation based on the re-sampling approach discussed in the text.

recorded, 12 g $m^{-2}$ $yr^{-1}$, which occurred from 2500 to 3500 cal BP. The late Holocene had a rapid increase in carbon accumulation from ~1500 cal BP onwards. However, this section of the records incorporates relatively undecomposed acrotelm peat and, as previously stated, should be interpreted with caution.

## DISCUSSION

**Bulk density and carbon content**

The carbon density of new records (Table 5) was within the estimates produced for the region by Chapman *et al*. (2009), but tending towards the lower end of the range. One reason for this could be the lower bulk density values we observed in the new records, which were around a third less than the means reported in Chapman *et al*. (2009), and much closer to the value for *Sphagnum* peat in the large global database compiled by Loisel *et al*. (2014), and previous studies of oceanic raised bog (Tomlinson & Davidson 2000). The carbon content of dry peat (Table 5) was in close agreement with the values reported in Chapman *et al*. (2009), with the mean values within one standard deviation of each other.

**General trends in carbon accumulation over time**

The time weighted carbon accumulation rate for the Flow Country was 16.3 g $m^{-2}$ $year^{-1}$ (including the top 50 cm for comparability purposes) for the new and re-analysed records. This is similar to the rate of carbon accumulation reported for oceanic blanket bog elsewhere, for example Patagonia (16 g $m^{-2}$ $yr^{-1}$ in Loisel & Yu 2013) and close to the mean value for northern peatlands (18.6 g $m^{-2}$ $yr^{-1}$ in Yu 2011). The decline in carbon accumulation rates from 8000 cal BP to 4000 BP, seen in both the new and inferred records (Figure 2, Figure 3), coincides with a gradual cooling of the climate in north-west Europe (Renssen *et al.* 2009). This pattern, i.e. high early Holocene carbon accumulation followed by declining rates in the mid-Holocene, is also seen in other published records from Scotland (Anderson 2002), and in compilations of long-term carbon accumulation from across northern peatlands generally (Vitt *et al.* 2000, Yu *et al.* 2009, Jones & Yu 2010, Loisel *et al.* 2014). This slowdown in mid-Holocene carbon accumulation rates has been attributed to a period of neoglacial cooling (Jones & Yu 2010, Loisel *et al.* 2014), which would be consistent with temperature reconstructions for north-west Europe (Mayewski *et al.* 2004, Renssen *et al.* 2009). Climatic cooling is thought to reduce peatland carbon accumulation due to a reduction in primary production which more than outweighs the parallel reduction in ecosystem


 DOI: 10.19189/MaP.2018.OMB.347

respiration (Jones & Yu 2010, Loisel *et al.* 2014). Declining carbon accumulation with lower temperatures is consistent with known changes in the transition from the Medieval Warm Period to the Little Ice Age (Mauquoy *et al.* 2002, Charman *et al.* 2013). Local pollen records from the Flow Country show declining tree cover during the transition from the early to mid-Holocene and is attributed in part to cooler conditions (Peglar 1979, Charman, 1994), which suggests the cooling trend inferred for north-west Europe also occurred within the Flow Country.

**Heterogeneity of carbon accumulation over time across records**

Changes in carbon accumulation over time are often found to be highly variable across sites (Anderson 2002, van Bellen *et al.* 2011, van der Linden *et al.* 2014, Swindles *et al.* 2017) and this is also apparent in our records (Figure 2). While a trend of declining mid-Holocene carbon accumulation is apparent in most records, there are a few exceptions. For example, GB2 and BADF both display the opposite trend, with mid-Holocene carbon accumulation relatively high between 4500 and 6000 cal BP. While the reason for this is not apparent it may relate to the hydrology of these sites. Van Bellen *et al*. (2011) and Belyea & Malmer (2004) found that carbon accumulation rates were controlled by plant species composition, which in turn was primarily driven by site hydrology, while Anderson (2002) found periods of rapid carbon uptake to be associated with lower humification and wetter climatic conditions (Anderson *et al.* 1998). It is possible that, for some sites, hydrological changes may counteract the effect of temperature at certain times, and this could explain the contradictory responses seen. However, human impacts such as peat cutting and burning cannot be ruled out, and are suspected to have affected some of our inferred records (Tipping 2007, Tipping *et al.* 2007a, 2008).

The direct role of temperature in regulating peat carbon accumulation is increasingly clear, with warmer annual temperatures generally promoting primary productivity more than decomposition (Charman *et al.* 2013, Klein *et al.* 2013, Munir *et al.* 2015). The role of hydrological change is less understood and the two are not entirely independent, with temperature a secondary control for peat surface moisture (Charman *et al.* 2009). Peatland carbon storage and uptake are sensitive to changes in water balance, with a theoretical 'optimal' water-table depth existing for peat accumulation (Belyea & Clymo 2001); above and below this threshold peatland carbon accumulation will be limited and the site may even become a source of C. This has been observed for peatland $CO_2$ fluxes, where ecosystem productivity (Euskirchen *et al.* 2014) and respiration (Euskirchen *et al.* 2014, Helfter *et al.* 2015) decline towards either extreme of the water-table range. Changes in hydrology are also known to be capable of causing rapid shifts in peatland carbon accumulation (Belyea & Malmer 2004, Yu 2006). This may explain some of the more extreme transitions in carbon accumulation observed here, such as those which occur between 3500 and 4500 cal BP for GB1, GB2, BADO and BADF and CRSLO (Figure 2).

There is considerable evidence from the north of Scotland to suggest that changes in water balance occurred between 3500 and 4500 cal BP, including fluctuating lake levels (Yu & Harrison 1995), changes in peat humification (Anderson *et al.* 1998, Tipping *et al.* 2008), changes in pollen indicative of moisture driven changes (Charman 1992, 1994), and the rapid expansion followed by the decline of *Pinus sylvestris* on previously open bog (Gear & Huntley 1991). It is thought that an initial drying phase occurred around 4405–4120 cal BP (Gear & Huntley 1991, Anderson 1998) followed by a transition to wetter conditions several hundred years later (Gear & Huntley 1991, Charman 1994, 1995; Anderson *et al.* 1998) at around 4020 to 3630 cal BP (Gear & Huntley 1991, Anderson 1998). The initiation of BRAEO and CATF around 4881 and 4287 cal BP would suggest that local conditions were likely to have been wet in the Flow Country at these times, as wetter conditions favour the lateral growth of blanket bog (Gallego-Sala *et al.* 2015).

A contradictory response in carbon accumulation is seen across sites around this time (Figure 2). Two records, BADF and BADO, display a marked decrease in carbon accumulation rate (by ~ 6 g $m^{-2}$ $yr^{-1}$) to 10–11 g $m^{-2}$ $yr^{-1}$ around 4000 cal BP. CRSLO and GB2 display an opposite trend, with carbon accumulation rate markedly increasing (by ~ 8 g $m^{-2}$ $yr^{-1}$) to 20–25 g $m^{-2}$ $yr^{-1}$ and GB1 displaying a similarly strong but somewhat asynchronous increase. A further three records (BRAEO, CATO, CRSLF) display weak declines, but the relatively poor chronology of these records limits the interpretations which can be made from them. The composite of the inferred records shows a slight increase in carbon accumulation at 4000 cal BP, and a reversal of the trend in declining carbon accumulation with time (Figure 3). It is possible local topography has influenced how the individual records responded, with CRSLO, GB1 and GB2 being located on moderately sloping ground, as opposed to BADO and BADF where the landscape is flatter and wetter. The influence of topography on the depth and vegetation of blanket bog has long been known (e.g. Aiton 1805), with peat development on


 DOI: 10.19189/MaP.2018.OMB.347

steep slopes limited by the inability to retain sufficient water. As such, topography is the primary determinant of bog cover in very humid climates (Gorham 1957, Bower 1961, Graniero & Price 1999). Consequently, areas of bog located on steep slopes are more likely to suffer erosion (Bower 1961), to be more sensitive to changes in water balance, and to suffer encroachment by shrub and heath communities with drier conditions (Graniero & Price 1999). Thus it should be expected that slope and topography will influence long-term carbon accumulation and its response to climate.

**Comparison with contemporary measurements of carbon sequestration**

Incidentally, sloping ground creates substantial technical challenges to measuring contemporary $CO_2$ fluxes using the eddy covariance technique (Papale *et al*. 2006, Etzold *et al*. 2010), potentially contributing to the poor understanding of carbon-terrain-climate interactions in blanket bog and highlighting one way in which it is difficult to make such comparisons across timescales. However, it is interesting to note that the maximum rate of carbon accumulation we report here (46.8 g $m^{-2}$ $year^{-1}$ at BADO around 4800 cal BP) is still considerably less than the contemporary ecosystem carbon sink recorded at Cross Lochs (99 g $m^{-2}$ $year^{-1}$ reported in Levy & Gray 2015). As noted by Ratcliffe *et al*. (2018), comparatively high contemporary carbon accumulation is a common phenomenon which has been observed across peatlands worldwide and there are a number of reasons why this may be the case. Continued measurements of contemporary carbon fluxes, coupled with good data on vegetation change, will be vital in order to reconcile this difference. Of particular importance is the question of whether periods of rapid carbon accumulation, such as we seem to be observing now (Levy & Gray 2015), will be followed by long periods of low accumulation, or whether a large loss of accumulated carbon can be expected in the near future.

## CONCLUSION

Our data are consistent with the idea that warmer conditions will promote greater carbon accumulation, but past records of carbon accumulation, presented here and elsewhere in the literature, also reveal the importance of other drivers, in particular changing water balance. Climate induced changes to water balance are likely to elicit different responses across different locations, which are harder to predict than temperature effects. The role of topography is likely to be an important, yet poorly understood, driver in the response of carbon to climate for blanket bog. The heterogeneity of changes in carbon accumulation over time, as inferred from these records and others, supports the need for a larger number of sites and a greater understanding of the factors which drive differences. The complex topography, altitude and microclimates of UK blanket bog provide the ideal opportunity to investigate such heterogeneity of response across both palaeo and contemporary time scales.

## ACKNOWLEDGEMENTS

This work was primarily funded by the Carnegie Trust for the Universities of Scotland (grant LG13STIR007), the Leverhulme Trust (RPG-2015-162), the British Ecological Society and the Royal Society. The research that generated the Gordonbush records was funded by SSE, ETP and EPSRC. We would also like to thank the RSPB, Patrick Sinclair, the Forestry Commission and SSE for granting access to the field sites and for help in retrieving the peat cores. Angela Creevy, David Braidwood and volunteers from Forsinard Flows NNR helped with the core collection while Prof. Stuart Gibb, Dr Chris Hayward and Norrie Russell provided valuable advice and assistance.

## AUTHOR CONTRIBUTIONS

The study was conceived by RJP and JLR. Fieldwork was conducted by JLR, TJS, BS, RA, ARA, RJP, SW and AH. Data compilation was conducted by JLR and RJP. Labwork was conducted by JLR, BS and TJS. RJP, RA, ARA, AN, DM, SW and AH secured funding and supervised students. Data analysis was conducted by JLR and RJP. JLR and RJP wrote the first draft of the manuscript to which all authors contributed.

## REFERENCES

Aiton, W. (1805) *A Treatise on the Origin, Qualities and Cultivation of Moss-Earth*. Niven, Napier and Khull, Glasgow, 45–59.

Anderson, D.E. (1998) A reconstruction of Holocene climatic changes from peat bogs in north-west Scotland. *Boreas*, 27(3), 208–224.

Anderson, D.E. (2002) Carbon accumulation and C/N ratios of peat bogs in north-west Scotland. *Scottish Geographical Journal*, 118(4), 323–341.


 DOI: 10.19189/MaP.2018.OMB.347

Anderson, D.E., Binney, H.A. & Smith, M.A. (1998) Evidence for abrupt climatic change in northern Scotland between 3900 and 3500 calendar years BP. *Holocene*, 8(1), 97–103.

Beilman, D.W., MacDonald, G.M., Smith, L.C. & Reimer, P.J. (2009) Carbon accumulation in peatlands of West Siberia over the last 2000 years. *Global Biogeochemical Cycles*, 23(1), 1–12.

Belokoptyov, I.E. & Beresnevich, V.V. (1955) Giktorf's peat borers. *Torfyanaya Promyshlennost*, 8, 9–10.

Belyea, L.R. (2009) Nonlinear dynamics of peatlands and potential feedbacks on the climate system. In: Baird, A.J., Belyea, L.R., Comas, X., Reeve, A.S. & Slater, L.D. (eds.) *Carbon Cycling in Northern Peatlands*, Geophysical Monograph 184, American Geophysical Union (AGU), Washington DC, 5–18.

Belyea, L.R. & Baird, A.J. (2006) Beyond "The limits to peat bog growth": Cross-scale feedback in peatland development. *Ecological Monographs*, 76(3), 299–322.

Belyea, L.R. & Clymo, R.S. (2001) Feedback control of the rate of peat formation. *Proceedings of the Royal Society of London B: Biological Sciences*, 268(1473), 1315–1321.

Belyea, L.R. & Malmer, N. (2004) Carbon sequestration in peatland: Patterns and mechanisms of response to climate change. *Global Change Biology*, 10(7), 1043–1052.

Berg, E.E., Hillman, K.M., Dial, R. & DeRuwe, A. (2009) Recent woody invasion of wetlands on the Kenai Peninsula Lowlands, south-central Alaska: a major regime shift after 18 000 years of wet *Sphagnum*-sedge peat recruitment. *Canadian Journal of Forest Research*, 39(11), 2033–2046.

Birse, E.L. (1971) *Assessment of Climatic Conditions in Scotland 3: The Bioclimatic Subregions Map and Explanatory Pamphlet*. Macaulay Institute for Soil Research, Aberdeen, 12 pp.

Blaauw, M. & Christen, A. (2011) Flexible paleoclimate age-depth models using an autoregressive gamma process. *Bayesian Analysis*, 6, 457–474.

Blanchet, G., Guillet, S., Calliari, B., Corona, C., Edvardsson, J., Stoffel, M. & Bragazza, L. (2017) Impacts of regional climatic fluctuations on radial growth of Siberian and Scots pine at Mukhrino mire (central-western Siberia). *Science of the Total Environment*, 574, 1209–1216.

Bower, M.M. (1961) The distribution of erosion in blanket peat bogs in the Pennines. *Transactions and Papers (Institute of British Geographers)*, 29, 17–30.

Bunting, M.J. & Tipping, R. (2004) Complex hydroseral vegetation succession and dryland pollen signals: a case study from northwest Scotland. *The Holocene*, 14(1), 53–63.

Chambers, F.M., Beilman, D.W. & Yu, Z. (2011) Methods for determining peat humification and for quantifying peat bulk density, organic matter and carbon content for palaeostudies of climate and peatland carbon dynamics. *Mires and Peat*, 7(7), 1–10.

Chapman, S.J., Bell, J., Donnelly, D. & Lilly, A. (2009) Carbon stocks in Scottish peatlands. *Soil Use and Management*, 25(2), 105–112.

Charman, D.J. (1990) *Origins and Development of the Flow Country Blanket Mire, Northern Scotland, with Particular Reference to Patterned Fens*. Unpublished PhD thesis, University of Southampton, 12–19.

Charman, D.J. (1992) Blanket mire formation at the Cross Lochs, Sutherland, northern Scotland. *Boreas*, 21(1), 53–72.

Charman, D.J. (1994) Late-glacial and Holocene vegetation history of the Flow Country, northern Scotland. *New Phytologist*, 127(1), 155–168.

Charman, D.J. (1995) Patterned fen development in northern Scotland: Hypothesis testing and comparison with ombrotrophic blanket peats. *Journal of Quaternary Science*, 10, 327–342.

Charman, D.J., Caseldine, C., Baker, A., Gearey, B., Hatton, J. & Proctor, C. (2001) Paleohydrological records from peat profiles and speleothems in Sutherland, northwest Scotland. *Quaternary Research*, 55(2), 223–234.

Charman, D.J., Barber, K.E., Blaauw, M., Langdon, P.G., Mauquoy, D., Daley, T.J., Hughes, P.D.M. & Karofeld, E. (2009) Climate drivers for peatland palaeoclimate records. *Quaternary Science Reviews*, 28(19–20), 1811–1819.

Charman, D.J., Beilman, D.W., Blaauw, M., Booth, R.K., Brewer, S., Chambers, F.M., Christen, J.A., Gallego-Sala, A., Harrison, S.P., Hughes, P.D.M., Jackson, S.T., Korhola, A., Mauquoy, D., Mitchell, F.J.G., Prentice, I.C., van der Linden, M., De Vleeschouwer, F., Yu, Z.C. & Alm, J. (2013) Climate-related changes in peatland carbon accumulation during the last millennium. *Biogeosciences*, 10(2), 929–944.

Charman, D.J., Amesbury, M.J., Hinchliffe, W., Hughes, P.D.M., Mallon, G., Blake, W.H., Daley, T.J., Gallego-Sala, A.V. & Mauquoy, D. (2015) Drivers of Holocene peatland carbon accumulation across a climate gradient in northeastern North America. *Quaternary Science Reviews*, 121, 110–119.

Chaudhary, N., Miller, P.A. & Smith, B. (2017) Modelling past, present and future peatland


 DOI: 10.19189/MaP.2018.OMB.347

carbon accumulation across the pan-Arctic. *Biogeosciences Discussions*, 1–45.

Clymo, R.S. (1984) The limits to peat bog growth. *Philosophical Transactions of the Royal Society of London B, Biological Sciences*, 303, 605–654.

Coulson, J.P., Bottrell, S.H. & Lee, J.A. (2005) Recreating atmospheric sulphur deposition histories from peat stratigraphy: Diagenetic conditions required for signal preservation and reconstruction of past sulphur deposition in the Derbyshire Peak District, UK. *Chemical Geology*, 218(3–4), 223–248.

Davies, A.L. (2011) Long-term approaches to native woodland restoration: palaeoecological and stakeholder perspectives on Atlantic forests of Northern Europe. *Forest Ecology and Management*, 261(3), 751–763.

De Vleeschouwer, F., Chambers, F.M. & Swindles, G.T. (2010) Coring and sub-sampling of peatlands for palaeoenvironmental research. *Mires and Peat*, 7(11), 1–10.

Dise, N.B. (2009) Peatland response to global change. *Science*, 326, 810–811.

Dugmore, A.J., Larsen, G.R. & Newton, A.J. (1995) Seven tephra isochrones in Scotland. *The Holocene*, 5(3), 257–266.

Etzold, S., Buchmann, N. & Eugster, W. (2010) Contribution of advection to the carbon budget measured by eddy covariance at a steep mountain slope forest in Switzerland. *Biogeosciences*, 7(8), 2461–2475.

Euskirchen, E.S., Edgar, C.W., Turetsky, M.R., Waldrop, M.P. & Harden, J.W. (2014) *Journal of Geophysical Research: Biogeosciences*, 119, 1576–1595.

Flanagan, L.B. & Syed, K.H. (2011) Stimulation of both photosynthesis and respiration in response to warmer and drier conditions in a boreal peatland ecosystem. *Global Change Biology*, 17(7), 2271–2287.

Frolking, S., Talbot, J., Jones, M.C., Treat, C.C., Kauffman, J.B., Tuittila, E.-S. & Roulet, N. (2011) Peatlands in the Earth's 21st century climate system. *Environmental Reviews*, 19, 371–396.

Gallego-Sala, A.V. & Prentice, C.I. (2013) Blanket peat biome endangered by climate change. *Nature Climate Change*, 3(2), 152–155.

Gallego-Sala, A.V., Charman, D.J., Harrison, S.P., Li, G. & Prentice, I.C. (2015) Climate-driven expansion of blanket bogs in Britain during the Holocene. *Climate of the Past*, 11(1), 4811–4832.

Gear, A.J. & Huntley, B. (1991) Rapid changes in the range limits of Scots pine 4000 years ago. *Science*, 251(4993), 544–547.

Goodrich, J.P., Campbell, D.I. & Schipper, L.A. (2017) Southern hemisphere bog persists as a strong carbon sink during droughts. *Biogeosciences*, 14 (20), 1–26.

Gorham, E. (1957) The development of peat lands. *The Quarterly Review of Biology*, 32(2), 145–166.

Goring, S., Williams, J.W., Blois, J.L., Jackson, S.T., Paciorek, C.J., Booth, R.K., Marlon, J.R., Blaauw, M. & Christen, J.A. (2012) Deposition times in the northeastern United States during the Holocene: Establishing valid priors for Bayesian age models. *Quaternary Science Reviews*, 48, 54–60.

Graniero, P.A. & Price, J.S. (1999) The importance of topographic factors on the distribution of bog and heath in a Newfoundland blanket bog complex. *Catena*, 36(3), 233–254.

Hedwall, P.O., Brunet, J. & Rydin, H. (2017) Peatland plant communities under global change: Negative feedback loops counteract shifts in species composition. *Ecology*, 98(1), 150–161.

Helfter, C., Campbell, C., Dinsmore, K.J., Drewer, J., Coyle, M., Anderson, M., Skiba, U., Nemitz, E., Billett, M.F. & Sutton, M.A. (2015) Drivers of long-term variability in $CO_2$ net ecosystem exchange in a temperate peatland. *Biogeosciences*, 12(6), 1799–1811.

Holden, J., Moody, C., Turner, T.E., McKenzie, R., Baird, A.J., Billett, M.F., Chapman, P.J., Dinsmore, K.J., Grayson, R.P., Andersen, R., Gee, C. & Dooling, G. (2017) Water-level dynamics in natural and artificial pools in blanket peatlands. *Hydrological Processes*, 32(4), 550–561.

Holmquist, J.R., Finkelstein, S.A., Garneau, M., Massa, C., Yu, Z. & MacDonald, G.M. (2016) A comparison of radiocarbon ages derived from bulk peat and selected plant macrofossils in basal peat cores from circum-arctic peatlands. *Quaternary Geochronology*, 31, 53–61.

Hughes, P.D.M., Lomas-Clarke, S.H., Schulz, J. & Barber, K.E. (2008) Decline and localized extinction of a major raised bog species across the British Isles: Evidence for associated land-use intensification. *Holocene*, 18(7), 1033–1043.

Jones, M.C. & Yu, Z. (2010) Rapid deglacial and early Holocene expansion of peatlands in Alaska. *Proceedings of the National Academy of Sciences of the United States of America (PNAS)*, 107, 7347–7352.

Jowsey, P.C. (1966) An improved peat sampler. *New Phytologist*, 65(2), 245–248.

Klein, E.S., Berg, E.E. & Dial, R. (2005) Wetland drying and succession across the Kenai Peninsula Lowlands, south-central Alaska. *Canadian Journal of Forest Research*, 35(8), 1931–1941.

Klein, E.S., Yu, Z. & Booth, R.K. (2013) Recent increase in peatland carbon accumulation in a thermokarst lake basin in Southwestern Alaska.


 DOI: 10.19189/MaP.2018.OMB.347

*Palaeogeography, Palaeoclimatology, Palaeoecology*, 392, 186–195.

Kottek, M., Grieser, J., Beck, C., Rudolf, B. & Rubel, F. (2006) World map of the Köppen-Geiger climate classification updated. *Meteorologische Zeitschrift*, 15(3), 259–263.

Laine, J., Vasander, H. & Sallantaus, T. (1995) Ecological effects of peatland drainage for forestry. *Environmental Reviews*, 3(3–4), 286–303.

Langdon, P.G. & Barber, K.E. (2004) Snapshots in time: precise correlations of peat-based proxy climate records in Scotland using mid-Holocene tephras. *The Holocene*, 14(1), 21–34.

Langdon, P.G., Barber, K.E. & Hughes, P.D.M. (2003) A 7500-year peat-based palaeoclimatic reconstruction and evidence for an 1100-year cyclicity in bog surface wetness from Temple Hill Moss, Pentland Hills, southeast Scotland. *Quaternary Science Reviews*, 22(2–4), 259–274.

Levy, P.E. & Gray, A. (2015) Greenhouse gas balance of a semi-natural peatbog in northern Scotland. *Environmental Research Letters*, 10, 094019, 1–11.

Lindsay, R. (2010) *Peatbogs and Carbon: a Critical Synthesis to Inform Policy Development in Oceanic Peat Bog Conservation and Restoration in the Context of Climate Change*. University of East London, 315 pp. Permanent URL: http://hdl.handle.net/10552/1144

Lindsay, R.A., Charman, D.J., Everingham, F., O'Reilly, R.M., Palmer, M.A., Rowell, T.A. & Stroud, D.A. (1988) *The Flow Country: The Peatlands of Caithness and Sutherland*. Edited by D.A. Ratcliffe and P.H. Oswald, Nature Conservancy Council, Peterborough, 174 pp. Available from Joint Nature Conservation Committee (JNCC) via http://jncc.defra.gov.uk/page-4281, accessed 07 Oct 2018.

Loisel, J. & Yu, Z. (2013) Holocene peatland carbon dynamics in Patagonia. *Quaternary Science Reviews*, 69, 125–141.

Loisel, J., Yu, Z., Beilman, D.W., Camill, P., Alm, J., Amesbury, M.J., Anderson, D., Andersson, S., Bochicchio, C., Barber, K., Belyea, L.R., Bunbury, J., Chambers, F.M., Charman, D.J., De Vleeschouwer, F., Fiałkiewicz-Kozieł, B., Finkelstein, S.A., Gałka, M., Garneau, M., Hammarlund, D., Hinchcliffe, W., Holmquist, J., Hughes, P., Jones, M.C., Klein, E.S., Kokfelt, U., Korhola, A., Kuhry, P., Lamarre, A., Lamentowicz, M., Large, D., Lavoie, M., MacDonald, G., Magnan, G., Makila, M., Mallon, G., Mathijssen, P., Mauquoy, D., McCarroll, J., Moore, T.R., Nichols, J., O'Reilly, B., Oksanen, P., Packalen, M., Peteet, D., Richard, P.J., Robinson, S., Ronkainen, T., Rundgren, M., Sannel, A.B.K., Tarnocai, C., Thom, T., Tuittila, E.-S., Turetsky, M., Valiranta, M., van der Linden, M., van Geel, B., van Bellen, S., Vitt, D., Zhao, Y. & Zhou, W. (2014) A database and synthesis of northern peatland soil properties and Holocene carbon and nitrogen accumulation. *The Holocene*, 24(9), 1028–1042.

Magnan, G. & Garneau, M. (2014) Climatic and autogenic control on Holocene carbon sequestration in ombrotrophic peatlands of maritime Quebec, eastern Canada. *The Holocene*, 24(9), 1054–1062.

Mauquoy, D. & Barber, K. (2002) Testing the sensitivity of the palaeoclimatic signal from ombrotrophic peat bogs in northern England and the Scottish Borders. *Review of Palaeobotany and Palynology*, 119(3), 219–240.

Mauquoy, D., Engelkes, T., Groot, M.H., Markesteijn, F., Oudejans, M.G., van der Plicht, J. & van Geel, B. (2002) High-resolution records of late-Holocene climate change and carbon accumulation in two north-west European ombrotrophic peat bogs. *Palaeogeography, Palaeoclimatology, Palaeoecology*, 186(3–4), 275–310.

Mayewski, P.A., Rohling, E.E., Stager, J.C., Karlén, W., Maasch, K.A., Meeker, L.D., Meyerson, E.A., Gasse, F., van Kreveld, S., Holmgren, K., Lee-Thorp, J., Rosqvist, G., Rack, F., Staubwasser, M., Schneider, R.R. & Steig, E.J. (2004) Holocene climate variability. *Quaternary Research*, 62(3), 243–255.

McClymont, E.L., Mauquoy, D., Yeloff, D., Broekens, P., Van Geel, B., Charman, D.J., Pancost, R.D., Chambers, F.P. & Evershed, R.P. (2008) The disappearence of *Sphagnum imbricatum* from Butterburn Flow, UK. *The Holocene*, 18(6), 991–1002.

Met Office (2014a) Scotland Rainfall (mm): Areal series, starting from 1910. Online at: https://www.metoffice.gov.uk/climate/uk/summaries/datasets, accessed 14 Oct 2018.

Met Office (2014b) Mean Temperature - Annual Average: 1971–2000. Online at: https://www.metoffice.gov.uk/public/weather/climate, accessed 14 Oct 2018.

Mitchell, M., Muftakhidinov, B. & Winchen, T. (2017) *Engauge Digitizer Software*. Online at: http://markummitchell.github.io/engauge-digitizer, accessed 14 Oct 2018.

Munir, T.M., Perkins, M., Kaing, E. & Strack, M. (2015) Carbon dioxide flux and net primary production of a boreal treed bog: Responses to warming and water-table-lowering simulations of climate change. *Biogeosciences*, 12, 1091–1111.


 DOI: 10.19189/MaP.2018.OMB.347

Newton, A.J., Dugmore, A.J. & Gittings, B.M. (2007) Tephrabase: tephrochronology and the development of a centralised European database. *Journal of Quaternary Science*, 22, 737–743.

Page, S.E. & Baird, A.J. (2016) Peatlands and global change: response and resilience. *Annual Review of Environment and Resources*, 41, 35–57.

Papale, D., Reichstein, M., Aubinet, M., Canfora, E., Bernhofer, C., Kutsch, W., Longdoz, B., Rambal, S., Valentini, R., Vesala, T. & Yakir, D. (2006) Towards a standardized processing of Net Ecosystem Exchange measured with eddy covariance technique: algorithms and uncertainty estimation. *Biogeosciences*, 3, 571–583.

Payne, R.J., Ratcliffe, J., Andersen, R. & Flitcroft, C.E. (2016) A meta-database of peatland palaeoecology in |Great Britain. *Palaeogeography, Palaeoclimatology, Palaeoecology*, 457, 389–395.

Peglar, S. (1979) A radiocarbon-dated pollen diagram from Loch of Winless, Caithness, north-east Scotland. *New Phytologist*, 82(1), 245–263.

Pellerin, S. & Lavoie, C. (2003) Recent expansion of jack pine in peatlands of southeastern Québec: A paleoecological study. *Ecoscience*, 10(2), 247–257.

Peteranna, M. (2012) *Braehour Forest Block Near Mybster, Caithness: Archaeological Walkover Survey - Summary of the Methodology and Results*. Ross & Cromarty Archaeological Services (RoCAS), Tore, Ross-shire, 23 pp. Online at: https://librarylink.highland.gov.uk/LLFiles/251990/full_251990.pdf, accessed 08 Oct 2018.

Ratcliffe, J. (2015) *Carbon Accumulation Rates Over the Holocene in Flow Country Peatlands and the Direct Comparison of Open and Afforested Peatland Carbon Stocks Using Tephrochronology*. Unpublished MSc thesis, University of Aberdeen, 120 pp.

Ratcliffe, J. & Payne, R.J. (2016) Palaeoecological studies as a source of peat depth data: A discussion and data compilation for Scotland. *Mires and Peat*, 18(13), 1–7.

Ratcliffe, J.L., Creevy, A., Andersen, R., Zarov, E., Gaffney, P.P.J., Taggart, M.A., Mazei, Y., Tsyganov, A.N., Rowson, J.G., Lapshina, E.D. & Payne, R.J. (2017) Ecological and environmental transition across the forested-to-open bog ecotone in a west Siberian peatland. *Science of the Total Environment*, 607–608, 816–828.

Ratcliffe, J., Andersen, R., Anderson, R., Newton, A., Campbell, D., Mauquoy, D. & Payne, R. (2018) Contemporary carbon fluxes do not reflect the long-term carbon balance for an Atlantic blanket bog. *Holocene*, 28(1), 140–149.

Reimer, P.J., Bard, E., Bayliss, A., Beck, J.W., Blackwell, P.G., Bronk Ramsey, C., Buck, C.E., Cheng, H., Edwards, R.L., Friedrich, M., Grootes, P.M., Guilderson, T.P., Haflidason, H., Hajdas, I., Hatté, C., Heaton, T.J., Hoffmann, D.L., Hogg, A.G., Hughen, K.A., Kaiser, K.F., Kromer, B., Manning, S.W., Niu, M., Reimer, R.W., Richards, D.A., Scott, E.M., Southon, J.R., Staff, R.A., Turney, C.S.M. & van der Plicht, J. (2013) IntCal13 and Marine13 radiocarbon age calibration curves 0–50,000 years cal BP. *Radiocarbon*, 55(4), 1869–1887.

Renssen, H., Seppä, H., Heiri, O., Roche, D.M., Goosse, H. & Fichefet, T. (2009) The spatial and temporal complexity of the Holocene thermal maximum. *Nature Geoscience*, 2(6), 411–414.

Robinson, D. (1987) Investigations into the Aukhorn Peat Mounds, Keiss, Caithness: Pollen, plant macrofossil and charcoal analyses. *New Phytologist*, 106, 185–200.

Scottish Government (2018) Scotland's soils. Online at: http://soils.environment.gov.scot/, accessed 20 Jun 2018.

Smith, B.A.V. (2016) *Assessment of Carbon and Nutrient Export from a Peatland Windfarm Construction Site*. Unpublished PhD thesis, University of Glasgow, 340 pp.

Smith, M.A. (1996) *The Role of Vegetation Dynamics and Human Activity in Landscape Changes through the Holocene in the Lairg Area, Sutherland, Scotland*. Unpublished PhD thesis, Royal Holloway, University of London, 125–247.

Stefanova, I., Van Leeuwen, J.F.N. & van der Knaap, W.O. (2008) 2. Loch Laxford (north-west Scotland, UK). *Grana*, 47(1), 78–79.

Sulman, B.N., Desai, A.R., Cook, B.D., Saliendra, N. & Mackay, D.S. (2009) Contrasting carbon dioxide fluxes between a drying shrub wetland in Northern Wisconsin, USA, and nearby forests. *Biogeosciences*, 6(6), 1115–1126.

Swindles, G.T., Lawson, I.T., Savov, I.P., Connor, C.B. & Plunkett, G. (2011) A 7000 yr perspective on volcanic ash clouds affecting northern Europe. *Geology*, 39(9), 887–890.

Swindles, G.T., Morris, P.J., Baird, A.J., Blaauw, M. & Plunkett, G. (2012) Ecohydrological feedbacks confound peat-based climate reconstructions. *Geophysical Research Letters*, 39(11), 2–5.

Swindles, G.T., Morris, P.J., Wheeler, J., Smith, M.W., Bacon, K.L., Turner, T.E., Headley, A. & Galloway, J.M. (2016) Resilience of peatland ecosystem services over millennial timescales: evidence from a degraded British bog. *Journal of Ecology*, 104(3), 621–636.

Swindles, G.T., Morris, P.J., Whitney, B., Galloway, J.M., Gałka, M., Gallego-Sala, A., Macumber,


 DOI: 10.19189/MaP.2018.OMB.347

A.L., Mullan, D., Smith, M.W., Amesbury, M.J. Roland, T.P., Sanei, H., Patterson, R.T., Sanderson, N., Parry, L., Charman, D.J., Lopez, O., Valderamma, E., Watson, E.J., Ivanovic, R.F., Valdes, P.J., Turner, T.E. & Lähteenoja, O. (2017) Ecosystem state shifts during long-term development of an Amazonian peatland. *Global Change Biology*. 24(2), 738–757.

Telford, R.J., Heegaard, E. & Birks, H.J.B. (2004) The intercept is a poor estimate of a calibrated radiocarbon age. *Holocene*, 14, 296–298.

Tipping, R. (2007) Blanket peat in the Scottish Highlands: timing, cause, spread and the myth of environmental determinism. *Biodiversity and Conservation*, 17(9), 2097–2113.

Tipping, R., Ashmore, P., Davies, A., Haggart, A., Moir, A., Newton, A., Sands, R., Skinner, T. & Tisdall, E. (2007a) Peat, pine stumps and people: interactions behind climate, vegetation change and human activity in wetland archaeology at Loch Farlary, north Scotland. In: Barber, J., Clark C., Cressey M., Crone A., Hale A., Henderson J., Housley R., Sands R. & Sheridan A. (eds.) *Archaeology from the Wetlands: Recent Perspectives*, Proceedings of the 11th WARP Conference, Edinburgh 2005 (WARP Occasional Paper 18), Society of Antiquaries of Scotland, Edinburgh, 157–164.

Tipping, R., Tisdall, E., Davies, A., Wilson, C. & Yendell, S. (2007b) Living with peat in the Flow Country: prehistoric farming communities and blanket peat spread at Oliclett, Caithness, northern Scotland. In: Barber, J., Clark C., Cressey, M., Crone, A., Hale, A., Henderson, J., Housley, R., Sands, R. & Sheridan, A. (eds.) *Archaeology from the Wetlands: Recent Perspectives*, Proceedings of the 11th WARP Conference, Edinburgh 2005 (WARP Occasional Paper 18), Society of Antiquaries of Scotland, Edinburgh, 165–173.

Tipping, R., Davies, A., McCulloch, R. & Tisdall, E. (2008) Response to late Bronze Age climate change of farming communities in north east Scotland. *Journal of Archaeological Science*, 35(8), 2379–2386.

Tomlinson, R.W. & Davidson, L. (2000) Estimates of carbon stores in four Northern Irish lowland raised bogs. *Suo*, 51(3), 169–179.

Turunen, J. (2003) Past and present carbon accumulation in undisturbed boreal and subarctic mires: A review. *Suo*, 54(1), 15–28.

van Bellen, S., Garneau, M. & Booth, R.K. (2011) Holocene carbon accumulation rates from three ombrotrophic peatlands in boreal Quebec, Canada: Impact of climate-driven ecohydrological change. *The Holocene*, 21(8), 1217–1231.

van der Linden, M., Heijmans, M.M.P.D. & van Geel, B. (2014) Carbon accumulation in peat deposits from northern Sweden to northern Germany during the last millennium. *Holocene*, 24(9), 1117–1125.

Vitt, D.H., Halsey, L.A., Bauer, I.E. & Campbell, C. (2000) Spatial and temporal trends in carbon storage of peatlands of continental western Canada through the Holocene. *Canadian Journal of Earth Sciences*, 37(5), 683–693.

Waddington, J.M., Morris, P.J., Kettridge, N., Granath, G., Thompson, D.K. & Moore, P.A. (2015) Hydrological feedbacks in northern peatlands. *Ecohydrology*, 8(1), 113–127.

Warren, C. (2000) "Birds, bogs and forestry" revisited: The significance of the Flow Country controversy. *Scottish Geographical Journal*, 116(4), 315–337.

Yu, G. & Harrison, S.P. (1995) Holocene changes in atmospheric circulation patterns as shown by lake status changes in northern Europe. *Boreas*, 24(3), 260–268.

Yu, Z. (2006) Holocene carbon accumulation of fen peatlands in boreal western Canada: A complex ecosystem response to climate variation and disturbance. *Ecosystems*, 9(8), 1278–1288.

Yu, Z. (2011) Holocene carbon flux histories of the world's peatlands: Global carbon-cycle implications. *The Holocene*, 21(5), 761–774.

Yu, Z., Beilman, D.W. & Jones, M.C. (2009) Sensitivity of northern peatland carbon dynamics to Holocene climate change. In: Baird, A.J., Belyea, L.R., Comas, X., Reeve, A.S. & Slater, L.D. (eds.) *Carbon Cycling in Northern Peatlands*, Geophysical Monograph 184, American Geophysical Union (AGU), Washington DC, 55–69.

Yu, Z., Loisel, J., Brosseau, D.P., Beilman, D.W. & Hunt, S.J. (2010) Global peatland dynamics since the Last Glacial Maximum. *Geophysical Research Letters*, 37(13), 1–5.

*Submitted 30 Mar 2018, revision 20 Jun 2018*
*Editor: Frank Chambers*

---

Author for correspondence: Joshua L Ratcliffe, Environmental Research Institute, North Highland College, University of the Highlands and Islands, Castle Street, Thurso, Caithness, KW14 7JD, Scotland, United Kingdom and Science & Engineering, University of Waikato, Private Bag 3105, Hamilton 3240, New Zealand. Email: jossratcliffe@gmail.com


 DOI: 10.19189/MaP.2018.OMB.347

# Appendix

Previously unpublished geochemical analyses from individual tephra shards found in peat cores in the north of Scotland. Geochemical analysis was carried out using a Cemeca SX100 electron probe microanalysis (EPMA) at the School of GeoSciences, University of Edinburgh. Operating conditions were: an accelerating voltage of 15 kV, with a beam current of 2 nA (Na, Mg, Al, Si, Ca, Fe and K) and 80 nA (Ti, Mn and P), and a beam diameter of 5 μm.

Table A1. Geochemistry from electronmicroprobe analysis of tephra shards found in the Cross Lochs Forest core at 122 cm, identified as Hekla 4.

| Shard | $Na_2O$ | $Al_2O_3$ | MgO | $SiO_2$ | $K_2O$ | CaO | FeO | $P_2O_5$ | $TiO_2$ | MnO | Total |
|---|---|---|---|---|---|---|---|---|---|---|---|
| 1 | 4.6216 | 14.325 | 0.6991 | 62.7544 | 1.7005 | 4.2478 | 9.1185 | 0.201 | 0.7014 | 0.291 | 98.6603 |
| 2 | 4.5717 | 14.2158 | 0.7687 | 62.7266 | 1.7298 | 4.3064 | 9.6748 | 0.2157 | 0.71 | 0.3058 | 99.2253 |
| 3 | 4.6206 | 14.205 | 0.8204 | 62.3069 | 1.5897 | 4.7575 | 8.8448 | 0.2822 | 0.8081 | 0.2802 | 98.5155 |
| 4 | 4.3903 | 13.9065 | 0.7213 | 62.0387 | 1.7684 | 4.5663 | 9.2786 | 0.2479 | 0.7021 | 0.2941 | 97.9142 |
| 5 | 4.0096 | 13.782 | 0.4917 | 63.9889 | 1.7484 | 4.4234 | 9.4916 | 0.1775 | 0.6319 | 0.2884 | 99.0333 |
| 6 | 4.732 | 13.7533 | 0.7144 | 62.4084 | 1.7312 | 4.2025 | 9.6605 | 0.2335 | 0.7267 | 0.281 | 98.4435 |
| 7 | 5.1065 | 13.7176 | 0.0121 | 69.7436 | 2.3886 | 2.2778 | 3.6534 | 0.0103 | 0.2046 | 0.142 | 97.2567 |
| 8 | 4.2966 | 13.5455 | 0.5355 | 62.9131 | 1.7926 | 4.3263 | 9.4829 | 0.1872 | 0.6447 | 0.3008 | 98.0251 |
| 9 | 4.8599 | 13.5385 | 0.5991 | 62.5996 | 1.8311 | 4.3603 | 9.1455 | 0.2192 | 0.6822 | 0.2864 | 98.1218 |
| 10 | 4.4373 | 13.4277 | 0.7255 | 62.8332 | 1.7057 | 4.1792 | 8.783 | 0.2472 | 0.7421 | 0.3013 | 97.3822 |
| 11 | 4.7784 | 13.3447 | 0.0268 | 71.72 | 2.5453 | 2.0896 | 3.3807 | 0.0078 | 0.1762 | 0.1319 | 98.2013 |
| 12 | 4.7723 | 13.3429 | 0.1944 | 67.556 | 2.0573 | 3.1971 | 6.0594 | 0.0677 | 0.3777 | 0.2188 | 97.8435 |
| 13 | 4.8934 | 13.2928 | 0.0845 | 68.4839 | 2.3235 | 2.843 | 5.1516 | 0.0436 | 0.2967 | 0.1964 | 97.6096 |
| 14 | 5.1514 | 13.2276 | 0.1138 | 69.1167 | 2.1628 | 2.9278 | 5.3619 | 0.0362 | 0.2974 | 0.1957 | 98.5914 |
| 15 | 4.9822 | 13.1034 | 0.03 | 70.9822 | 2.5118 | 2.3045 | 3.909 | 0.0146 | 0.216 | 0.139 | 98.1928 |
| 16 | 5.0472 | 13.0798 | 0.0681 | 69.0402 | 2.4261 | 2.4619 | 4.1555 | 0.0225 | 0.2355 | 0.1513 | 96.688 |
| 17 | 4.8092 | 12.8118 | 0.031 | 73.2542 | 2.8311 | 1.3202 | 1.8925 | 0.0033 | 0.0892 | 0.064 | 97.1065 |
| 18 | 4.6536 | 12.7982 | 0.0186 | 74.0671 | 3.0182 | 1.3601 | 2.073 | 0.0075 | 0.0907 | 0.0721 | 98.1591 |
| 19 | 4.8775 | 12.7494 | 0.0449 | 68.8564 | 2.3256 | 2.6024 | 4.3545 | 0.0348 | 0.2693 | 0.1712 | 96.2861 |
| 20 | 4.8879 | 12.6824 | 0.0052 | 73.2103 | 2.901 | 1.4823 | 1.8279 | 0.0042 | 0.0893 | 0.0969 | 97.1874 |
| 21 | 4.6817 | 12.635 | -0.0001 | 73.7135 | 2.9369 | 1.225 | 2.0705 | 0.0029 | 0.0936 | 0.0803 | 97.4394 |
| 22 | 4.575 | 12.5639 | -0.0089 | 72.8208 | 2.8242 | 1.3102 | 2.1034 | 0.0052 | 0.0916 | 0.0779 | 96.3632 |
| 23 | 4.6499 | 12.5418 | -0.0013 | 72.343 | 2.7678 | 1.3535 | 1.9909 | 0.0059 | 0.0905 | 0.0893 | 95.8314 |
| 24 | 4.7345 | 12.5403 | 0.0073 | 74.3139 | 2.8917 | 1.2789 | 1.9454 | -0.0037 | 0.0824 | 0.0847 | 97.8755 |
| 25 | 4.9702 | 12.4807 | 0.0297 | 72.2397 | 2.7587 | 1.4211 | 1.8541 | 0.0011 | 0.0927 | 0.0811 | 95.929 |
| 26 | 4.4498 | 12.4343 | 0.0222 | 73.7809 | 2.8758 | 1.3598 | 1.7938 | 0.0004 | 0.094 | 0.0876 | 96.8985 |
| 27 | 5.1636 | 12.4001 | 0.0245 | 70.8473 | 2.6196 | 1.938 | 3.1579 | 0.0011 | 0.1495 | 0.1125 | 96.414 |
| 28 | 4.876 | 12.3724 | 0.014 | 73.1629 | 2.9519 | 1.3483 | 2.0829 | 0.015 | 0.0869 | 0.0748 | 96.9851 |
| 29 | 5.0255 | 12.2104 | 0.0393 | 69.3579 | 2.3024 | 2.5352 | 3.8124 | 0.0362 | 0.2188 | 0.1585 | 95.6966 |
| 30 | 4.8223 | 12.1982 | 0.0084 | 74.7827 | 3.0191 | 1.1268 | 2.1036 | 0.0004 | 0.0841 | 0.0766 | 98.2222 |
| 31 | 4.5301 | 12.1546 | -0.0118 | 73.6532 | 2.8926 | 1.4327 | 2.0889 | 0.0033 | 0.0931 | 0.093 | 96.9296 |
| 32 | 4.7833 | 12.0455 | 0.001 | 73.3157 | 2.9166 | 1.3317 | 1.8359 | 0.0115 | 0.0892 | 0.0821 | 96.4122 |
| 33 | 4.4215 | 11.8802 | 0.0193 | 76.7084 | 3.0965 | 0.9375 | 0.9521 | 0.0137 | 0.0886 | 0.0557 | 98.1735 |
| 34 | 4.6722 | 11.4675 | 0.0116 | 73.628 | 2.912 | 1.3873 | 2.147 | 0.0096 | 0.0883 | 0.0889 | 96.4123 |


 DOI: 10.19189/MaP.2018.OMB.347

Table A2. Geochemistry from electronmicroprobe analysis of tephra shards found in the Catanach Forest core at 97 cm, identified as Hekla 4.

| Shard | $Na_2O$ | $Al_2O_3$ | MgO | $SiO_2$ | $K_2O$ | CaO | FeO | $P_2O_5$ | $TiO_2$ | MnO | Total |
|---|---|---|---|---|---|---|---|---|---|---|---|
| 1 | 4.2242 | 14.6462 | 0.7994 | 61.5684 | 1.6312 | 4.6715 | 9.2768 | 0.3116 | 0.7876 | 0.2907 | 98.2076 |
| 2 | 4.8101 | 14.6065 | 0.627 | 62.7105 | 1.8137 | 4.4076 | 9.2616 | 0.2476 | 0.7065 | 0.2916 | 99.4826 |
| 3 | 1.7677 | 14.5522 | 0.3042 | 66.4709 | 1.9839 | 3.6382 | 7.1651 | 0.1299 | 0.5162 | 0.2445 | 96.7728 |
| 4 | 4.2444 | 14.4458 | 0.5915 | 62.7318 | 1.7592 | 4.2686 | 9.265 | 0.2226 | 0.6765 | 0.2682 | 98.4735 |
| 5 | 4.3876 | 14.4372 | 0.7284 | 61.7508 | 1.6403 | 4.3951 | 9.0582 | 0.2774 | 0.7132 | 0.2763 | 97.6644 |
| 6 | 4.8468 | 14.4039 | 0.9077 | 62.5491 | 1.6751 | 4.2406 | 9.1977 | 0.3311 | 0.8101 | 0.2834 | 99.2453 |
| 7 | 5.1824 | 14.3477 | -0.003 | 73.5185 | 2.3326 | 1.8181 | 1.2643 | 0.0118 | 0.1007 | 0.0675 | 98.6407 |
| 8 | 5.0728 | 14.1051 | 0.5585 | 60.5548 | 1.7208 | 4.0371 | 12.9895 | 0.2094 | 0.8607 | 0.2914 | 100.3999 |
| 9 | 4.9238 | 13.9212 | 0.5193 | 62.2967 | 1.7077 | 4.0209 | 8.5775 | 0.2081 | 0.6324 | 0.2908 | 97.0984 |
| 10 | 4.6781 | 13.8583 | 0.8084 | 62.7435 | 1.4844 | 4.3488 | 9.5123 | 0.2755 | 0.7392 | 0.2985 | 98.7471 |
| 11 | 4.8852 | 13.8207 | 0.8897 | 61.0658 | 1.6109 | 4.5376 | 9.727 | 0.3126 | 0.7886 | 0.2825 | 97.9206 |
| 12 | 4.6542 | 13.6304 | 0.7089 | 61.7714 | 1.6772 | 4.4741 | 9.3418 | 0.2562 | 0.7179 | 0.2863 | 97.5183 |
| 13 | 4.379 | 13.6259 | 0.674 | 62.3823 | 1.8261 | 4.3576 | 9.4595 | 0.2444 | 0.7189 | 0.3022 | 97.9699 |
| 14 | 4.5567 | 13.5743 | 0.04 | 70.4863 | 2.7089 | 2.0762 | 3.2394 | 0.0198 | 0.1787 | 0.1399 | 97.0201 |
| 15 | 4.5133 | 13.5472 | 0.7771 | 61.7625 | 1.6851 | 4.2547 | 9.0255 | 0.245 | 0.7245 | 0.2858 | 96.8207 |
| 16 | 5.1063 | 13.4918 | 0.0242 | 75.2462 | 2.827 | 1.437 | 2.184 | 0.0079 | 0.0957 | 0.0822 | 100.5023 |
| 17 | 4.1861 | 13.486 | 0.4108 | 66.2307 | 2.0377 | 3.617 | 7.3781 | 0.1724 | 0.5902 | 0.2732 | 98.3823 |
| 18 | 4.7984 | 13.4355 | 0.109 | 67.7678 | 2.3251 | 3.0127 | 5.2738 | 0.056 | 0.3146 | 0.1954 | 97.2883 |
| 19 | 4.3492 | 13.3423 | 0.2605 | 65.4205 | 2.0476 | 3.2693 | 6.3866 | 0.0967 | 0.4118 | 0.2096 | 95.7941 |
| 20 | 5.2779 | 13.2913 | 0.206 | 66.3001 | 2.0052 | 3.4564 | 6.3547 | 0.0591 | 0.3822 | 0.2217 | 97.5548 |
| 21 | 4.821 | 12.8817 | 0.0287 | 72.9355 | 2.8457 | 1.3491 | 1.9297 | 0.0155 | 0.0927 | 0.089 | 96.9887 |
| 22 | 4.908 | 12.7449 | 0.0165 | 73.0358 | 2.9192 | 1.3912 | 2.2649 | 0.0073 | 0.0863 | 0.0827 | 97.4567 |
| 23 | 4.6816 | 12.7399 | -0.0133 | 74.5915 | 2.9174 | 1.2042 | 1.6318 | 0.0118 | 0.0962 | 0.0766 | 97.9377 |
| 24 | 4.6789 | 12.6077 | 0.0129 | 74.3054 | 2.914 | 1.3007 | 1.9795 | 0.0097 | 0.0889 | 0.0879 | 97.9855 |
| 25 | 2.7037 | 12.5517 | 0.0074 | 74.5215 | 3.1214 | 1.5203 | 2.1766 | 0.0107 | 0.1175 | 0.0932 | 96.8238 |
| 26 | 4.0626 | 12.4087 | 0.0171 | 74.4819 | 2.8529 | 1.4211 | 1.871 | -0.0004 | 0.0912 | 0.0821 | 97.2885 |
| 27 | 4.8139 | 12.3764 | 0.0061 | 74.904 | 2.7616 | 1.3508 | 1.7336 | -0.0094 | 0.0922 | 0.0753 | 98.1046 |
| 28 | 4.1649 | 12.3741 | 0.0341 | 76.2925 | 2.6844 | 1.2598 | 1.8061 | 0.0064 | 0.0747 | 0.0659 | 98.763 |
| 29 | 4.4889 | 12.3372 | 0.0106 | 74.0151 | 2.8809 | 1.2549 | 1.9652 | 0.003 | 0.0956 | 0.0735 | 97.125 |
| 30 | 4.7742 | 12.3194 | 0.0163 | 73.8969 | 2.8321 | 1.388 | 1.7693 | 0.0089 | 0.0965 | 0.0927 | 97.1943 |
| 31 | 4.72 | 12.2711 | 0.0341 | 73.3555 | 2.8721 | 1.3628 | 1.9034 | 0.0008 | 0.0863 | 0.0772 | 96.6831 |
| 32 | 4.5234 | 12.2514 | 0.0308 | 73.5252 | 2.8372 | 1.3549 | 1.9485 | 0 | 0.0976 | 0.0757 | 96.6447 |
| 33 | 4.2827 | 12.1123 | 0.0225 | 73.1828 | 3.0576 | 1.3085 | 1.9862 | 0.0096 | 0.0887 | 0.0651 | 96.116 |
| 34 | 4.5957 | 12.1051 | -0.0104 | 73.7116 | 3.0995 | 0.9091 | 1.3452 | 0.0079 | 0.0917 | 0.061 | 95.9164 |
| 35 | 4.7102 | 12.0818 | -0.008 | 74.6335 | 2.9692 | 1.3371 | 2.1292 | 0.0044 | 0.088 | 0.0962 | 98.0417 |
| 36 | 4.5766 | 12.0391 | 0.0113 | 73.0905 | 2.8099 | 1.4334 | 1.9389 | 0.0132 | 0.0848 | 0.0808 | 96.0786 |
| 37 | 4.2273 | 12.0263 | 0.0274 | 73.9597 | 2.9193 | 1.3577 | 1.8525 | 0.0003 | 0.1035 | 0.0717 | 96.5457 |
| 38 | 4.7456 | 11.8706 | 0.0227 | 73.9825 | 3.0087 | 1.2822 | 1.944 | 0.0093 | 0.0883 | 0.0734 | 97.0274 |
| 39 | 4.8035 | 11.6498 | 0.0232 | 73.0701 | 2.8064 | 1.353 | 2.1303 | 0.0185 | 0.0907 | 0.0764 | 96.022 |
| 40 | 4.5807 | 11.097 | 0.0341 | 75.4818 | 2.9011 | 1.3282 | 1.7901 | 0.0089 | 0.0847 | 0.0695 | 97.3763 |


 DOI: 10.19189/MaP.2018.OMB.347

Table A3. Geochemistry from electronmicroprobe analysis of tephra shards found in the Braehour open core at 102 cm, identified as Hekla 4.

| Shard | $SiO_2$ | $TiO_2$ | $Al_2O_3$ | FeO | MnO | MgO | CaO | $Na_2O$ | $K_2O$ | $P_2O_5$ | Total |
|---|---|---|---|---|---|---|---|---|---|---|---|
| 1 | 71.4127 | 0.094 | 12.6292 | 2.036 | 0.0816 | 0.0232 | 1.2701 | 4.9315 | 2.7502 | 0.0088 | 95.2372 |
| 2 | 72.4119 | 0.0888 | 12.6629 | 1.9985 | 0.0927 | 0.0455 | 1.349 | 4.8331 | 2.7155 | 0.0053 | 96.2032 |
| 3 | 64.687 | 0.4072 | 13.761 | 6.3295 | 0.2396 | 0.2065 | 3.3823 | 5.1973 | 2.0704 | 0.0913 | 96.3719 |
| 4 | 72.5742 | 0.0848 | 12.606 | 1.8515 | 0.0907 | 0.0246 | 1.269 | 4.9956 | 2.9069 | 0.0121 | 96.4153 |
| 5 | 72.6753 | 0.1111 | 13.0829 | 1.9828 | 0.0839 | 0.0173 | 1.3659 | 4.7352 | 2.7249 | 0.0083 | 96.7876 |
| 6 | 73.2008 | 0.096 | 12.7114 | 1.8431 | 0.0863 | 0.0101 | 1.2772 | 4.9673 | 2.8508 | -0.0039 | 97.0392 |
| 7 | 73.642 | 0.0979 | 13.3257 | 1.9744 | 0.0821 | 0.0112 | 1.4261 | 4.7086 | 2.8379 | 0.0104 | 98.1163 |
| 8 | 73.5316 | 0.0893 | 13.235 | 2.0258 | 0.0822 | 0.0357 | 1.3626 | 4.961 | 2.8769 | 0.0112 | 98.2114 |
| 9 | 73.4037 | 0.0902 | 13.5215 | 1.7906 | 0.0806 | 0.0438 | 1.3303 | 5.1325 | 2.8305 | 0.007 | 98.2308 |
| 10 | 67.5862 | 0.3375 | 14.7713 | 5.1839 | 0.1972 | 0.1939 | 3.0194 | 5.0264 | 2.0777 | 0.0597 | 98.4534 |
| 11 | 74.6564 | 0.0931 | 13.0446 | 1.9592 | 0.0829 | 0.0134 | 1.4117 | 4.9142 | 2.6769 | 0.0176 | 98.8701 |
| 12 | 74.1145 | 0.0956 | 13.4076 | 1.8247 | 0.0791 | 0.021 | 1.3257 | 5.1889 | 2.8747 | -0.0028 | 98.9292 |
| 13 | 74.2018 | 0.0928 | 13.1542 | 2.025 | 0.0789 | -0.0039 | 1.4 | 5.4523 | 2.861 | 0.0063 | 99.2685 |
| 14 | 74.9283 | 0.0999 | 13.3005 | 1.968 | 0.0721 | 0.0111 | 1.39 | 4.7823 | 2.9829 | 0.0126 | 99.5476 |
| 15 | 74.2965 | 0.0911 | 13.6216 | 1.8213 | 0.0751 | 0.0188 | 1.451 | 5.4858 | 2.7779 | 0.0067 | 99.6458 |
| 16 | 74.1593 | 0.0899 | 13.608 | 2.0335 | 0.0821 | 0.0013 | 1.4649 | 5.3092 | 2.8994 | 0.0081 | 99.6559 |
| 17 | 73.111 | 0.099 | 13.8474 | 2.7629 | 0.1004 | 0.0567 | 1.8474 | 5.6569 | 2.3233 | 0.006 | 99.8111 |
| 18 | 68.9723 | 0.2951 | 15.291 | 4.8773 | 0.2034 | 0.088 | 2.8369 | 5.1803 | 2.1134 | 0.0405 | 99.8983 |
| 19 | 70.801 | 0.2061 | 14.6038 | 3.9178 | 0.1468 | 0.042 | 2.3109 | 5.4747 | 2.3843 | 0.0126 | 99.9 |
| 20 | 64.9646 | 0.5411 | 14.5327 | 8.0806 | 0.2993 | 0.3916 | 3.9472 | 5.1964 | 1.9122 | 0.1285 | 99.9941 |
| 21 | 74.8326 | 0.0957 | 13.5788 | 1.9389 | 0.0694 | 0 | 1.4385 | 5.4013 | 2.7837 | 0.0116 | 100.1506 |
| 22 | 76.1176 | 0.0766 | 13.0458 | 1.8162 | 0.0823 | 0.0503 | 1.3434 | 4.8694 | 2.9158 | 0.0064 | 100.3237 |
| 23 | 64.2805 | 0.6295 | 14.4589 | 8.69 | 0.2929 | 0.5024 | 4.4135 | 5.0932 | 1.8029 | 0.1626 | 100.3264 |
| 24 | 74.9199 | 0.1037 | 13.7936 | 2.0499 | 0.0714 | -0.0047 | 1.4112 | 5.282 | 2.8492 | 0.0151 | 100.4914 |
| 25 | 65.9973 | 0.6746 | 15.2218 | 7.6351 | 0.2428 | 0.4935 | 3.7887 | 5.479 | 1.9436 | 0.2077 | 101.6842 |
| 26 | 76.4013 | 0.0762 | 14.2765 | 1.7431 | 0.0822 | 0.0289 | 1.371 | 5.0368 | 2.846 | 0.0082 | 101.8702 |


 DOI: 10.19189/MaP.2018.OMB.347

Table A4. Geochemistry from electronmicroprobe analysis of tephra shards found in the Bad a' Cheo Forest core at 114 cm, identified as Hekla 4.

| Shard | $SiO_2$ | $TiO_2$ | $Al_2O_3$ | FeO | MnO | MgO | CaO | $Na_2O$ | $K_2O$ | $P_2O_5$ | Total |
|---|---|---|---|---|---|---|---|---|---|---|---|
| 1 | 73.806 | 0.0912 | 12.8201 | 1.6277 | 0.0896 | 0.0383 | 1.3023 | 4.906 | 3.0212 | 0.0123 | 97.7147 |
| 2 | 73.133 | 0.1007 | 12.687 | 2.0035 | 0.0734 | 0.0259 | 1.3252 | 4.9524 | 2.7455 | -0.0031 | 97.0434 |
| 3 | 63.3296 | 0.7063 | 15.556 | 8.5523 | 0.2757 | 0.7053 | 4.3555 | 5.0474 | 1.6979 | 0.237 | 100.4631 |
| 4 | 76.2989 | 0.0867 | 13.5226 | 1.2191 | 0.0741 | 0.0135 | 1.1457 | 4.8208 | 2.8658 | -0.0014 | 100.046 |
| 5 | 62.9813 | 0.7274 | 15.1443 | 8.9435 | 0.3002 | 0.7227 | 4.4182 | 4.811 | 1.7988 | 0.2454 | 100.0927 |
| 6 | 71.9973 | 0.1931 | 14.2822 | 3.626 | 0.1382 | 0.0238 | 2.0939 | 5.372 | 2.5509 | 0.015 | 100.2924 |
| 7 | 74.2555 | 0.099 | 13.5539 | 1.898 | 0.0703 | 0.0267 | 1.3537 | 5.1457 | 2.8688 | 0.0081 | 99.2797 |
| 8 | 68.6742 | 0.2559 | 13.3638 | 4.323 | 0.181 | 0.058 | 2.5758 | 5.4137 | 2.2417 | 0.0382 | 97.1254 |
| 9 | 73.1187 | 0.0865 | 13.5851 | 1.9589 | 0.0883 | 0.0077 | 1.3349 | 5.0411 | 2.9414 | 0.0042 | 98.1669 |
| 10 | 73.4872 | 0.0726 | 12.7621 | 1.8627 | 0.0764 | 0.0367 | 1.3354 | 4.4362 | 2.8235 | 0.0095 | 96.9024 |
| 11 | 63.1539 | 0.7309 | 15.0259 | 9.268 | 0.2809 | 0.7365 | 4.5191 | 4.7676 | 1.813 | 0.2587 | 100.5544 |
| 12 | 70.7543 | 0.2084 | 13.4454 | 3.663 | 0.148 | 0.037 | 2.1867 | 5.3663 | 2.4221 | 0.0352 | 98.2664 |
| 13 | 73.6445 | 0.1507 | 14.6106 | 2.7734 | 0.1063 | 0.0849 | 1.8232 | 5.6471 | 2.5707 | 0.0175 | 101.4288 |
| 14 | 74.4566 | 0.0928 | 13.0755 | 1.858 | 0.0666 | 0.0196 | 1.4058 | 5.1903 | 2.8108 | 0.0119 | 98.988 |
| 15 | 72.7891 | 0.0919 | 13.4871 | 2.0144 | 0.0782 | 0.0246 | 1.3174 | 4.9939 | 2.7827 | 0.0088 | 97.5881 |
| 16 | 73.3414 | 0.0985 | 13.5867 | 1.9031 | 0.0749 | 0.0289 | 1.3519 | 4.7866 | 2.8736 | 0.014 | 98.0597 |
| 17 | 74.2175 | 0.0938 | 13.2118 | 2.1624 | 0.0817 | 0.0101 | 1.3725 | 5.5476 | 2.8036 | 0.0042 | 99.5051 |
| 18 | 74.5517 | 0.0812 | 12.5617 | 1.678 | 0.0749 | 0.0343 | 1.2811 | 4.8321 | 2.6517 | 0.0021 | 97.749 |
| 19 | 73.8368 | 0.0906 | 12.8741 | 1.8523 | 0.0746 | 0.044 | 1.343 | 5.1034 | 2.759 | 0.0039 | 97.9818 |
| 20 | 63.9481 | 0.6661 | 14.919 | 8.5064 | 0.275 | 0.588 | 4.2358 | 5.2176 | 1.8505 | 0.2014 | 100.4079 |

Table A5. Geochemistry from electronmicroprobe analysis of tephra shards found in the Bad a' Cheo Forest core at 122 cm, identified as Lairg A.

| Shard | $SiO_2$ | $TiO_2$ | $Al_2O_3$ | FeO | MnO | MgO | CaO | $Na_2O$ | $K_2O$ | $P_2O_5$ | Total |
|---|---|---|---|---|---|---|---|---|---|---|---|
| 1 | 72.4257 | 0.077 | 12.7577 | 1.563 | 0.0543 | 0.049 | 1.2697 | 4.9233 | 2.5491 | 0.0154 | 95.6843 |
| 2 | 73.9154 | 0.084 | 12.7029 | 1.638 | 0.055 | 0.064 | 1.3621 | 4.9353 | 2.6537 | 0.0046 | 97.415 |
| 3 | 72.4601 | 0.0809 | 11.8517 | 1.6331 | 0.0575 | 0.0202 | 1.3408 | 4.5132 | 2.6714 | 0.0074 | 94.6364 |
| 4 | 72.2267 | 0.072 | 12.4574 | 1.5271 | 0.0609 | 0.0289 | 1.2593 | 4.5947 | 2.5292 | 0.0091 | 94.7653 |
| 5 | 73.1633 | 0.0792 | 12.9474 | 1.5864 | 0.0623 | 0.0328 | 1.3887 | 5.0086 | 2.6636 | 0.012 | 96.9443 |
| 6 | 73.9765 | 0.0756 | 13.1788 | 1.6948 | 0.0632 | 0.0344 | 1.3425 | 4.6526 | 2.8137 | 0.0045 | 97.8365 |
| 7 | 72.1896 | 0.0696 | 12.1069 | 1.5003 | 0.0638 | 0.0447 | 1.2876 | 4.7018 | 2.6315 | 0.0035 | 94.5993 |
| 8 | 73.462 | 0.0815 | 12.4324 | 1.7499 | 0.0652 | 0.0272 | 1.3375 | 5.1047 | 2.6869 | 0.0131 | 96.9604 |
| 9 | 72.9777 | 0.0884 | 12.3385 | 1.5743 | 0.0669 | 0.0289 | 1.2693 | 4.8545 | 2.733 | -0.0021 | 95.9293 |
| 10 | 72.5682 | 0.0673 | 12.3255 | 1.5305 | 0.0684 | 0.0267 | 1.3265 | 4.5639 | 2.6854 | 0.0098 | 95.1722 |
| 11 | 73.8026 | 0.0775 | 12.2649 | 1.4983 | 0.0693 | 0.0387 | 1.3414 | 4.4673 | 2.687 | 0.0109 | 96.2579 |
| 12 | 73.5934 | 0.0772 | 13.0971 | 1.5784 | 0.074 | 0.02 | 1.2706 | 4.6835 | 2.7889 | 0.0043 | 97.1873 |
| 13 | 74.5517 | 0.0812 | 12.5617 | 1.678 | 0.0749 | 0.0343 | 1.2811 | 4.8321 | 2.6517 | 0.0021 | 97.749 |
| 14 | 72.6551 | 0.0785 | 12.1051 | 1.4721 | 0.0762 | 0.0465 | 1.2876 | 4.3302 | 2.7688 | 0.0043 | 94.8242 |
| 15 | 72.8548 | 0.0722 | 12.1988 | 1.7171 | 0.0788 | 0.0434 | 1.3047 | 4.7118 | 2.6702 | 0.0078 | 95.6595 |
| 16 | 75.5344 | 0.0752 | 12.8787 | 1.8865 | 0.0789 | 0.0324 | 1.326 | 4.6246 | 2.9225 | -0.0018 | 99.3574 |
| 17 | 73.7053 | 0.0793 | 12.3718 | 1.7231 | 0.0806 | 0.0368 | 1.3437 | 4.8787 | 2.7623 | 0.0032 | 96.9847 |
| 18 | 73.9582 | 0.076 | 12.6148 | 1.8003 | 0.0841 | 0.0242 | 1.2748 | 4.6855 | 2.8298 | 0.0056 | 97.3533 |
| 19 | 74.5675 | 0.0795 | 12.6405 | 1.4383 | 0.0852 | 0.0028 | 1.3899 | 4.6014 | 2.7159 | 0.0092 | 97.5301 |


 DOI: 10.19189/MaP.2018.OMB.347

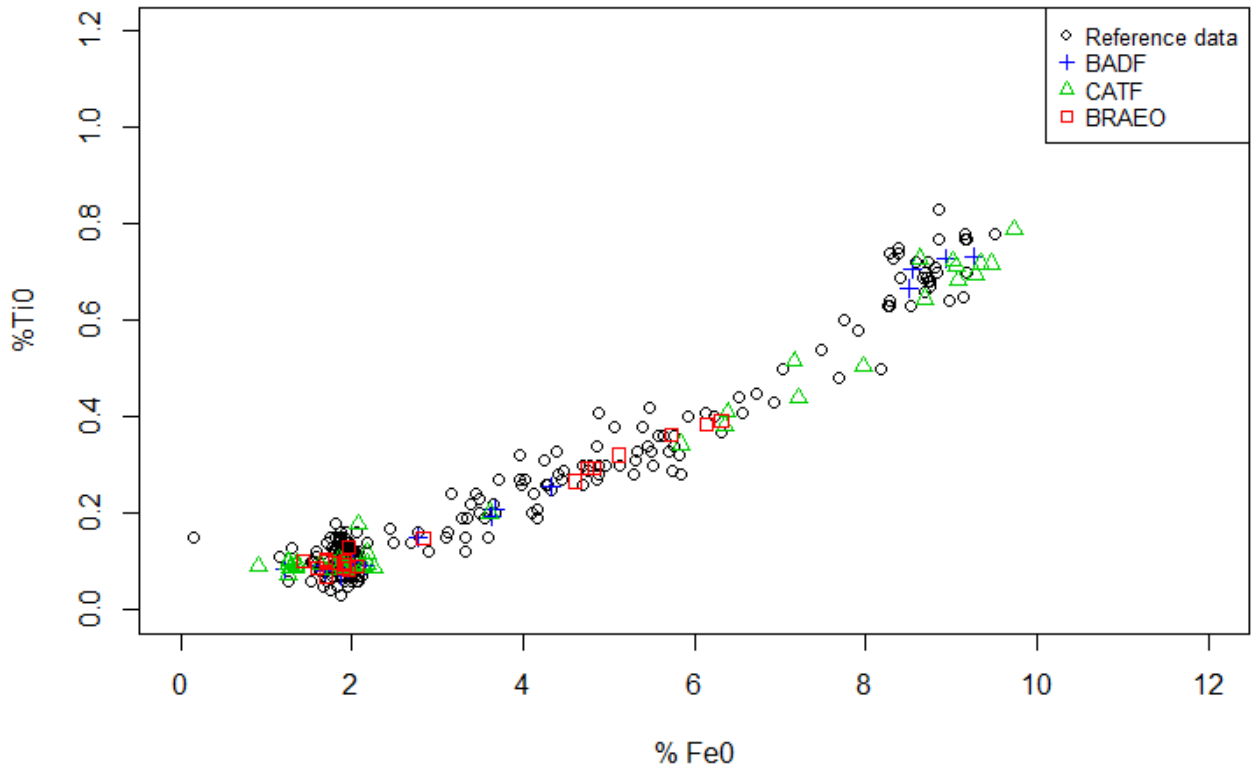


Figure A1. % TiO and FeO of reference Hekla 4 shards from Tephrabase (Newton *et al*. 2007), displayed as black circles, compared with shards from BADF 114.4, CATF 97.4 and BRAEO 102.4.

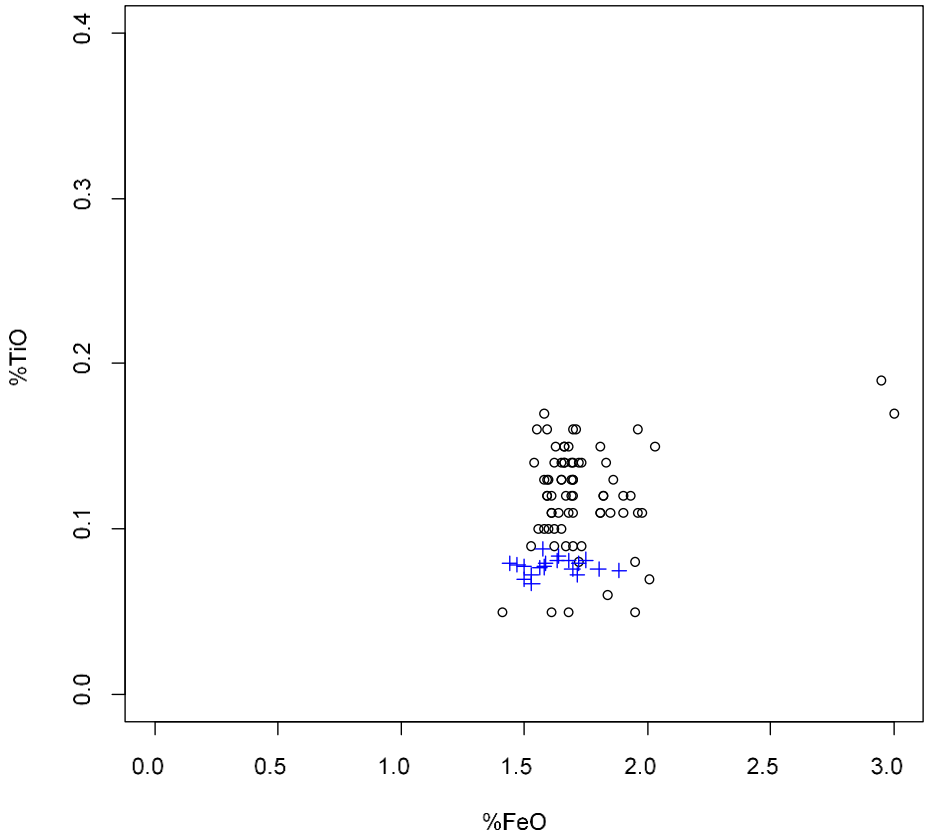


Figure A2. % TiO and FeO of reference Lairg A shards from Tephrabase (Newton *et al*. 2007), displayed as black circles, compared with shards from BADF 228.


 DOI: 10.19189/MaP.2018.OMB.347

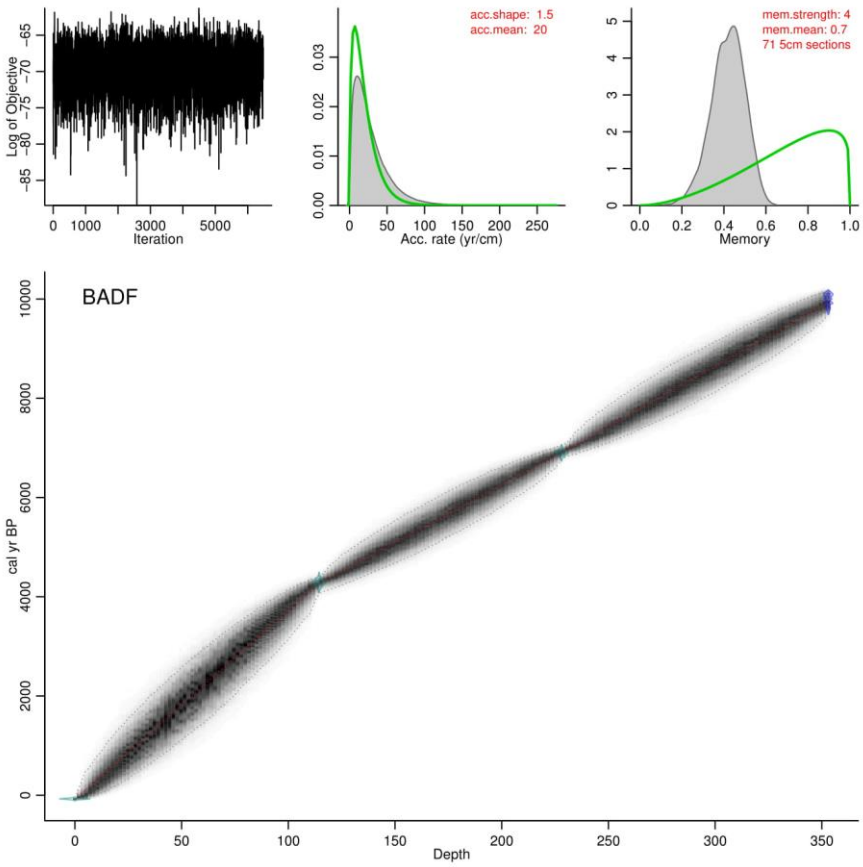


Figure A3a. Age-depth model produced in BACON for BADF.

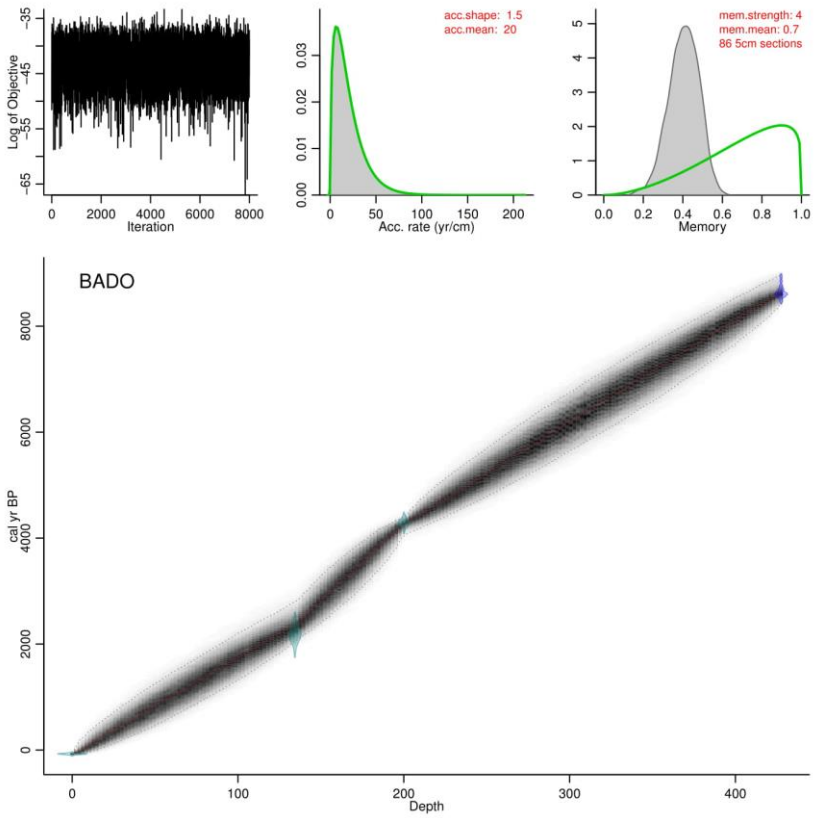


Figure A3b. Age-depth model produced in BACON for BADO.

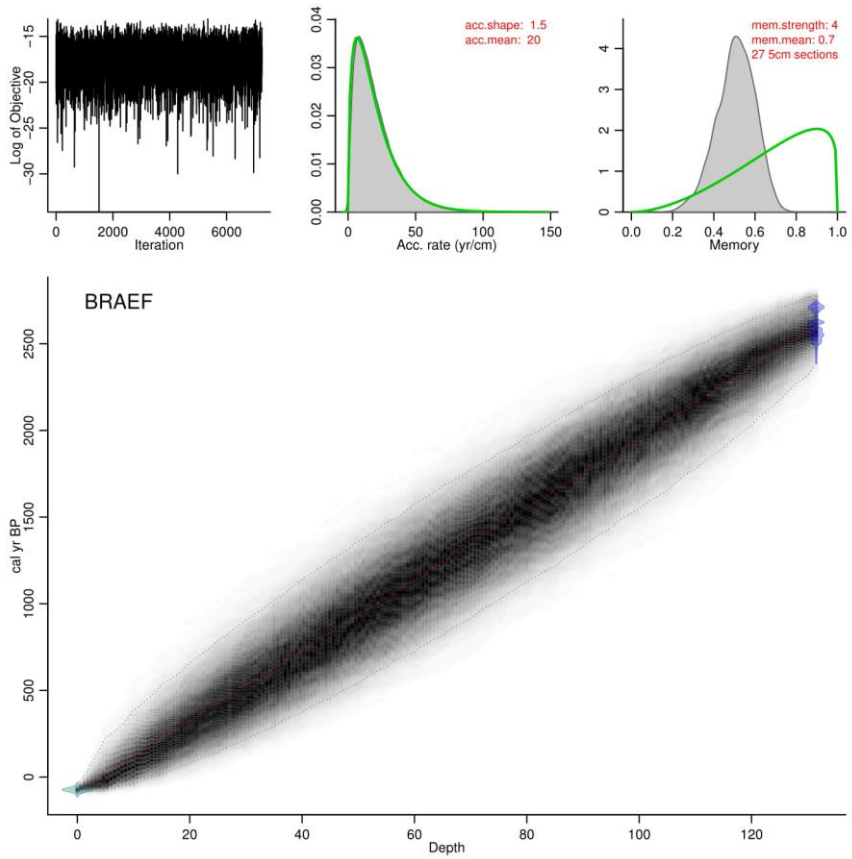


Figure A3c. Age-depth model produced in BACON for BRAEF.

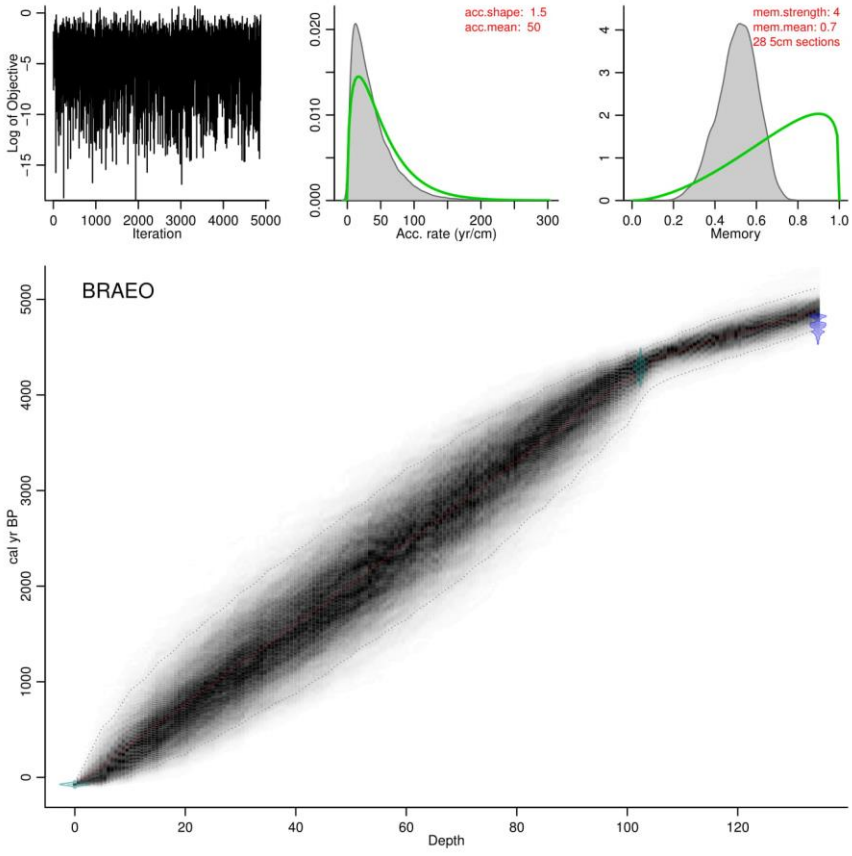


Figure A3d. Age-depth model produced in BACON for BRAEO.

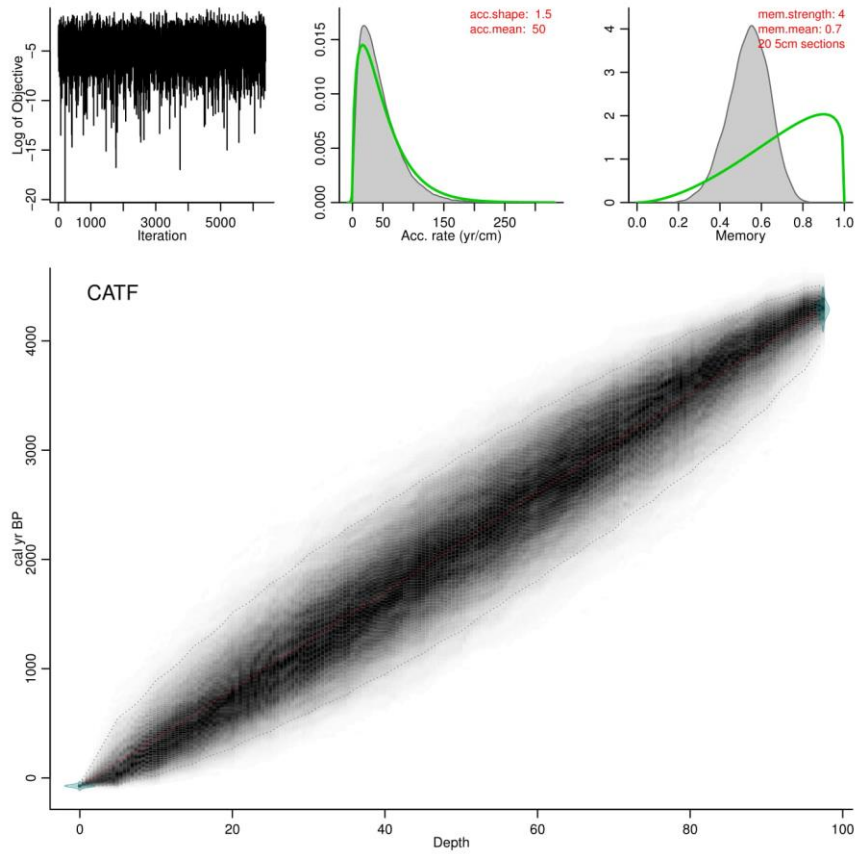


Figure A3e. Age-depth model produced in BACON for CATF.

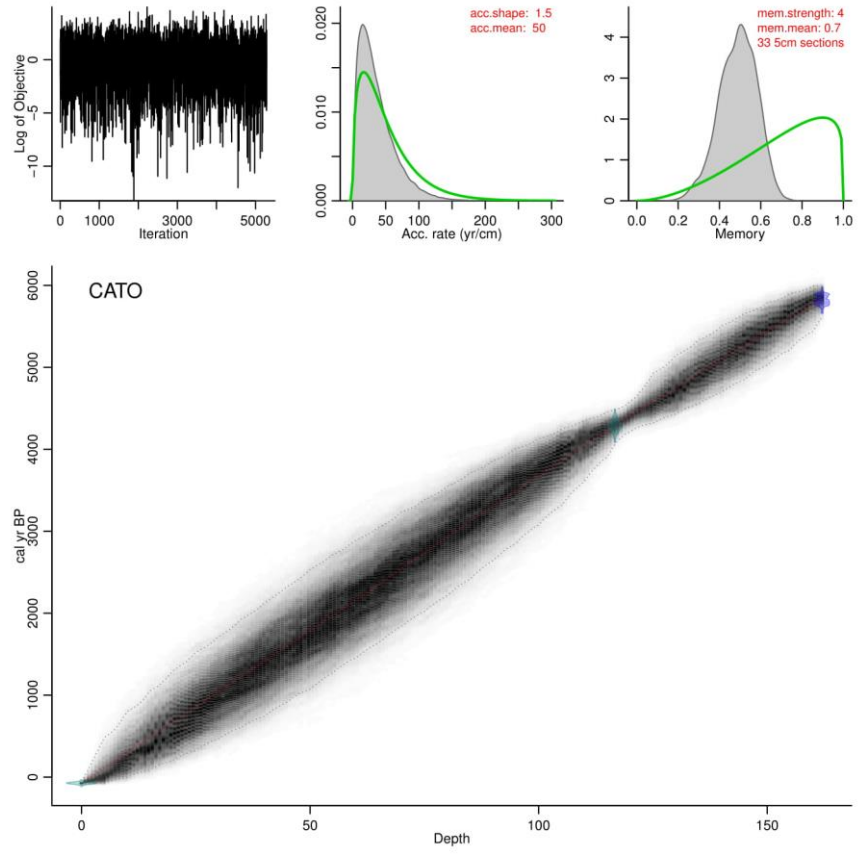


Figure A3f. Age-depth model produced in BACON for CATO.

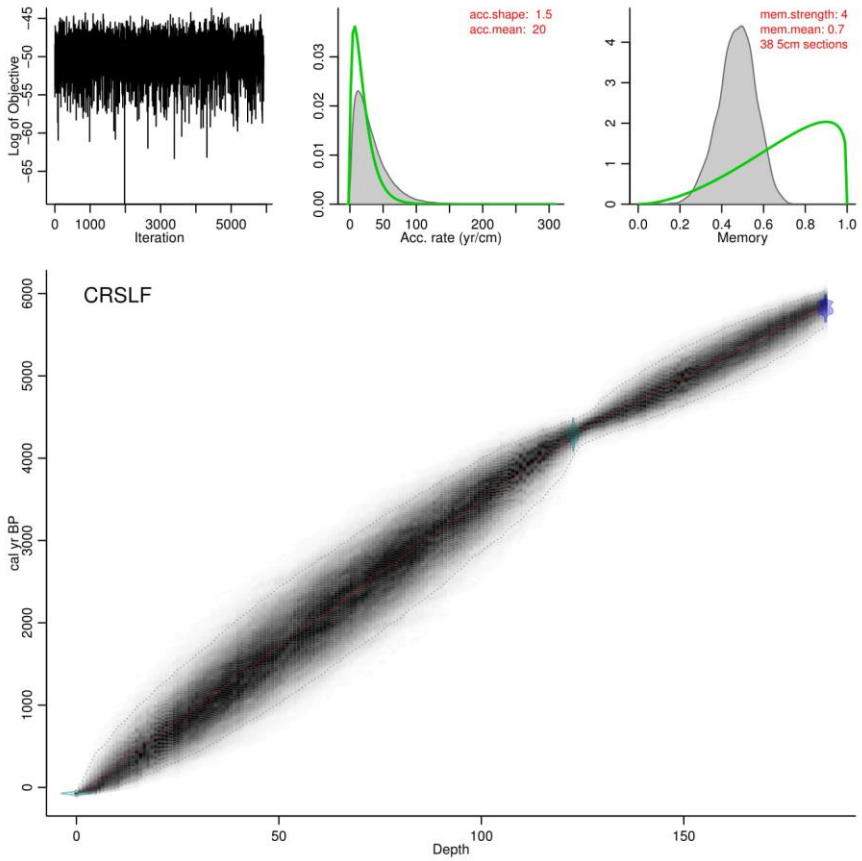


Figure A3g. Age-depth model produced in BACON for CRSLF.

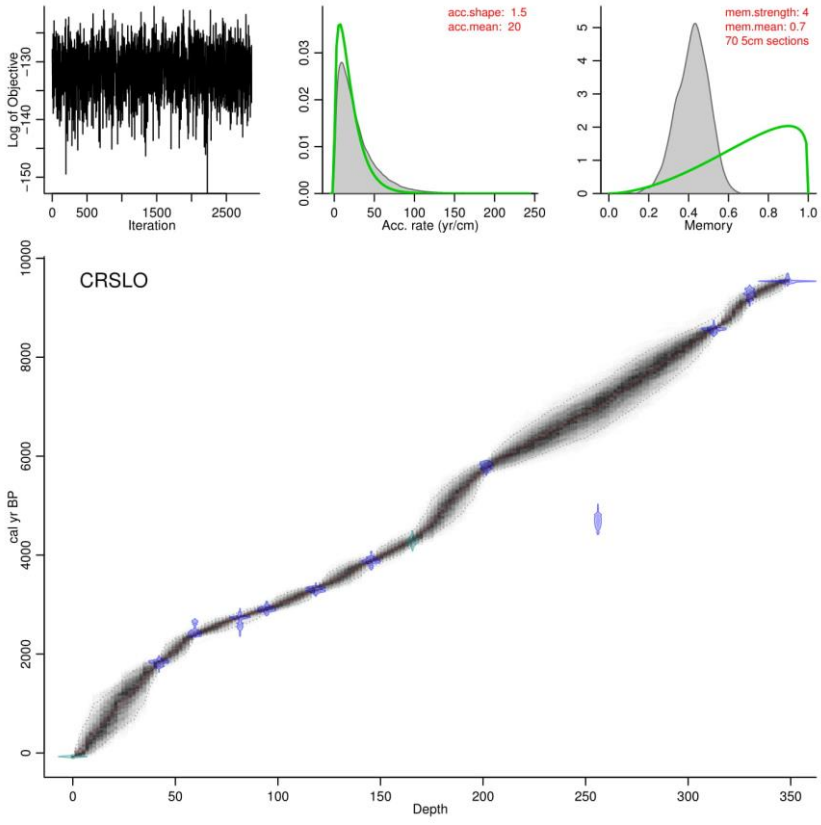


Figure A3h. Age-depth model produced in BACON for CRSLO.

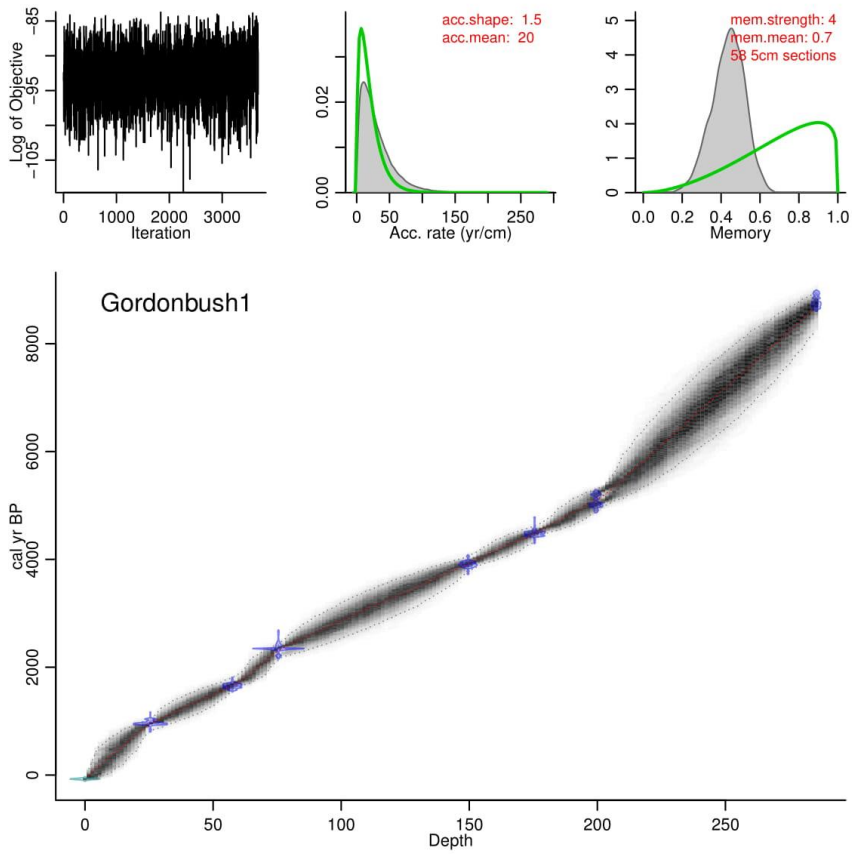


Figure A3i. Age-depth model produced in BACON for GB1.

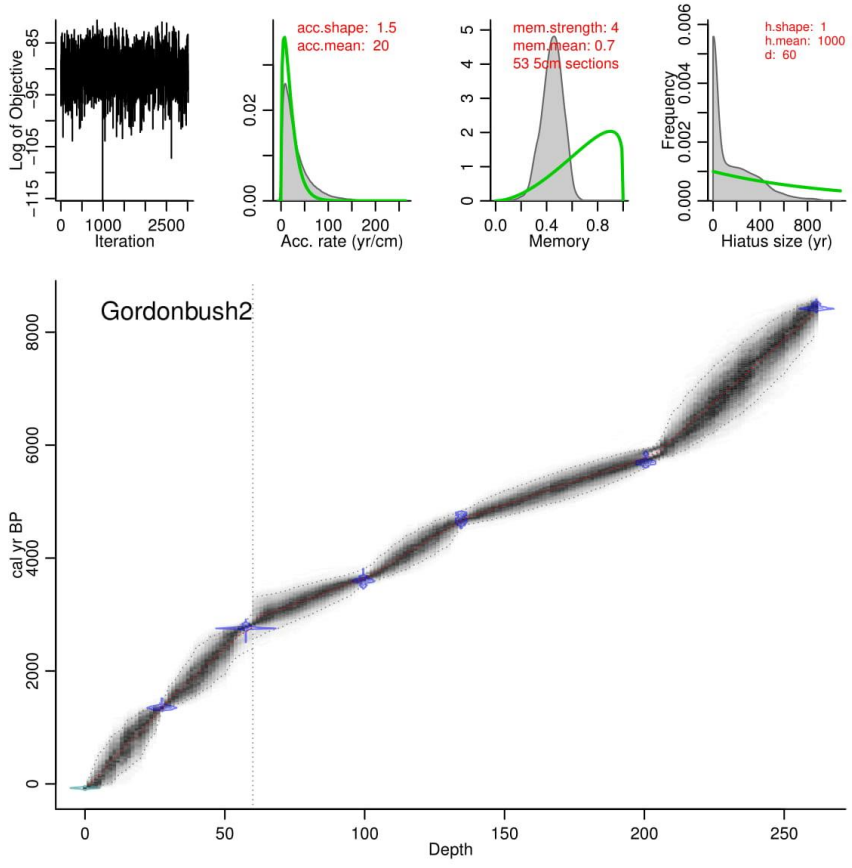


Figure A3j. Age-depth model produced in BACON for GB2.

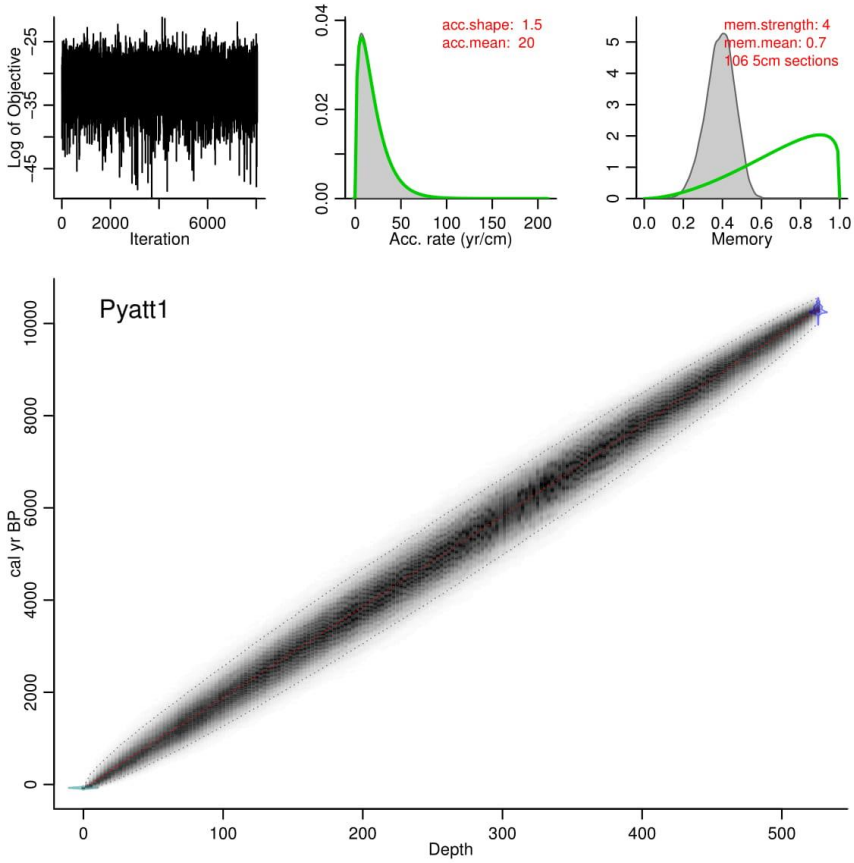


Figure A3k. Age-depth model produced in BACON for BADP1.

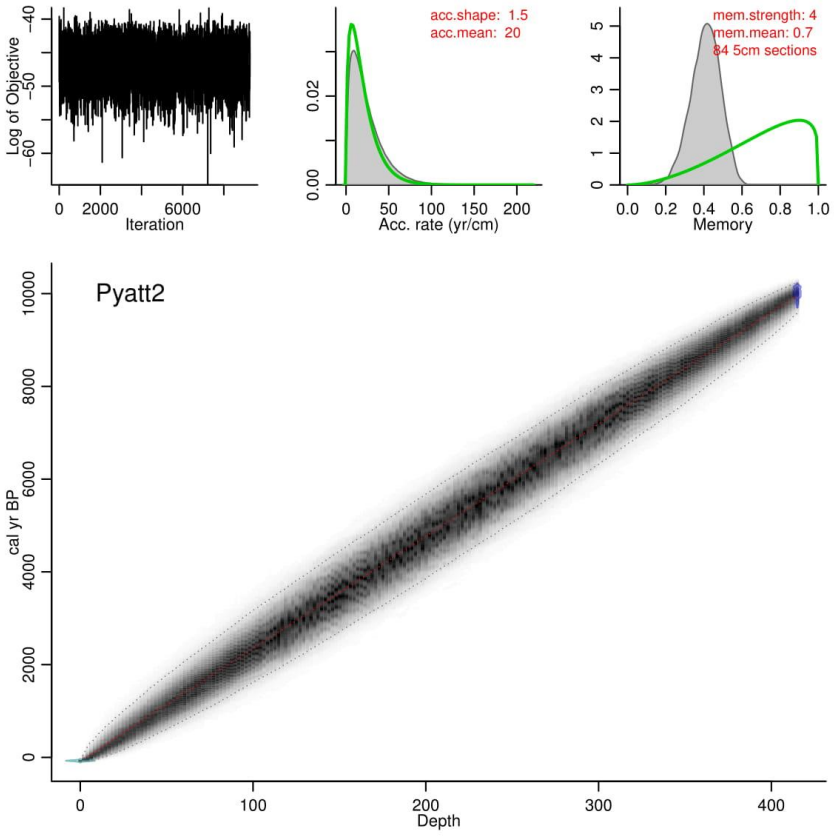


Figure A3l. Age-depth model produced in BACON for BADP2.

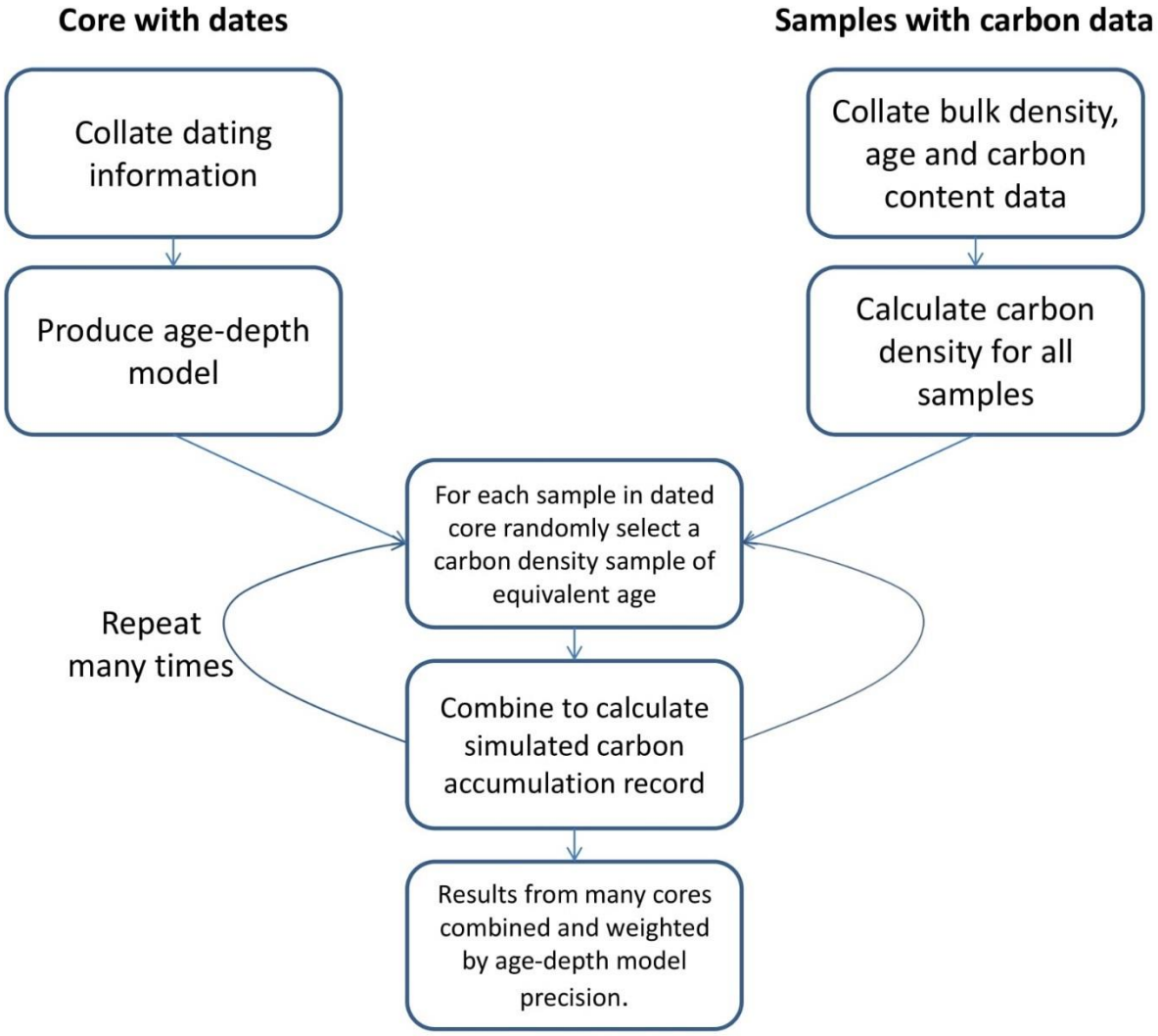


Figure A4. Schematic diagram of the process used to produce inferred records of carbon accumulation.


 DOI: 10.19189/MaP.2018.OMB.347